HXR intensity, directivity and polarization in solar flares

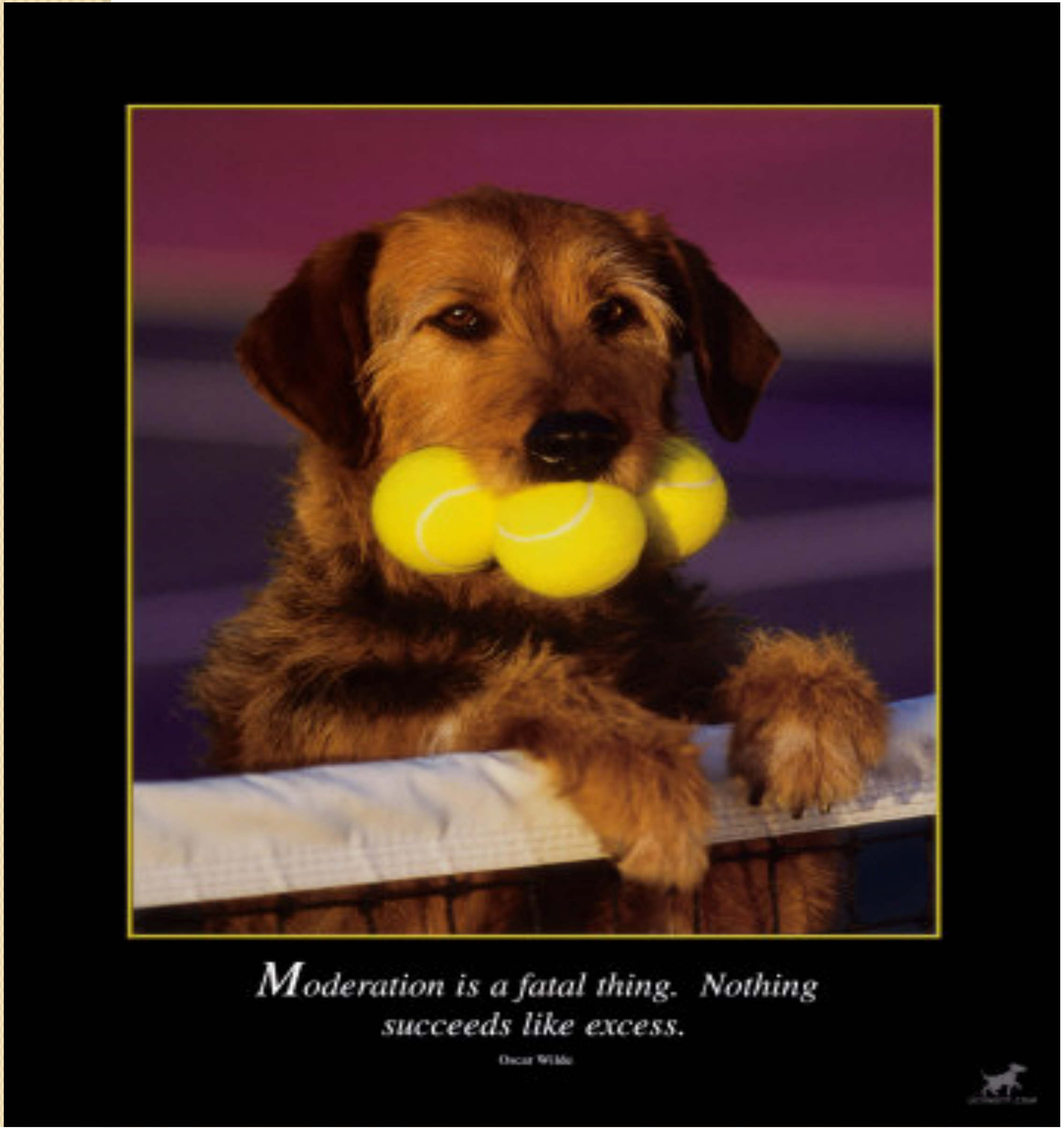

Valentina Zharkova

Zharkova et al,
1995, A&A
Siversky&Zharkova
A&A, 2009,
Zharkova et al,
2010, 2011, A&A

Solar flare mechanisms

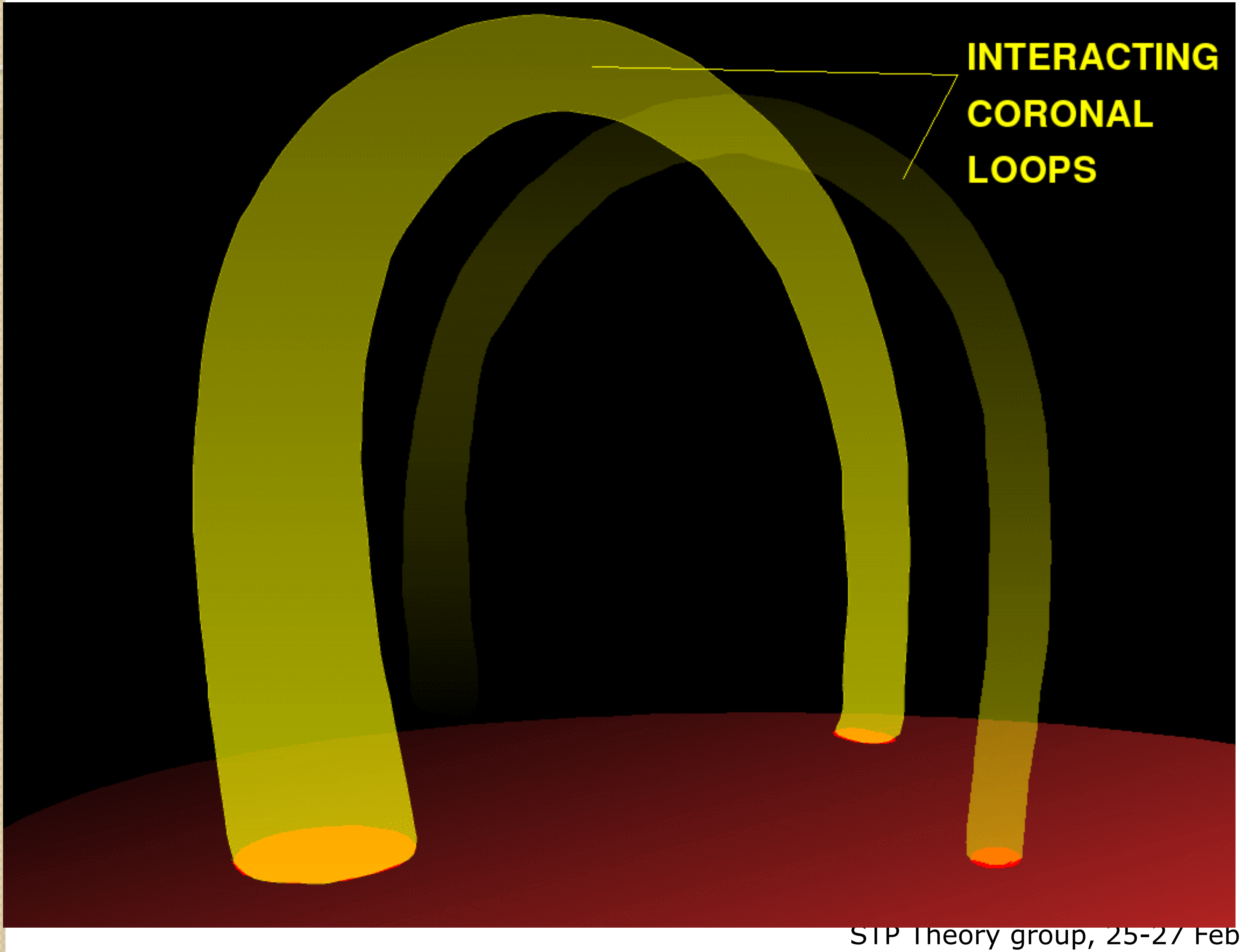

Particle acceleration in solar flares

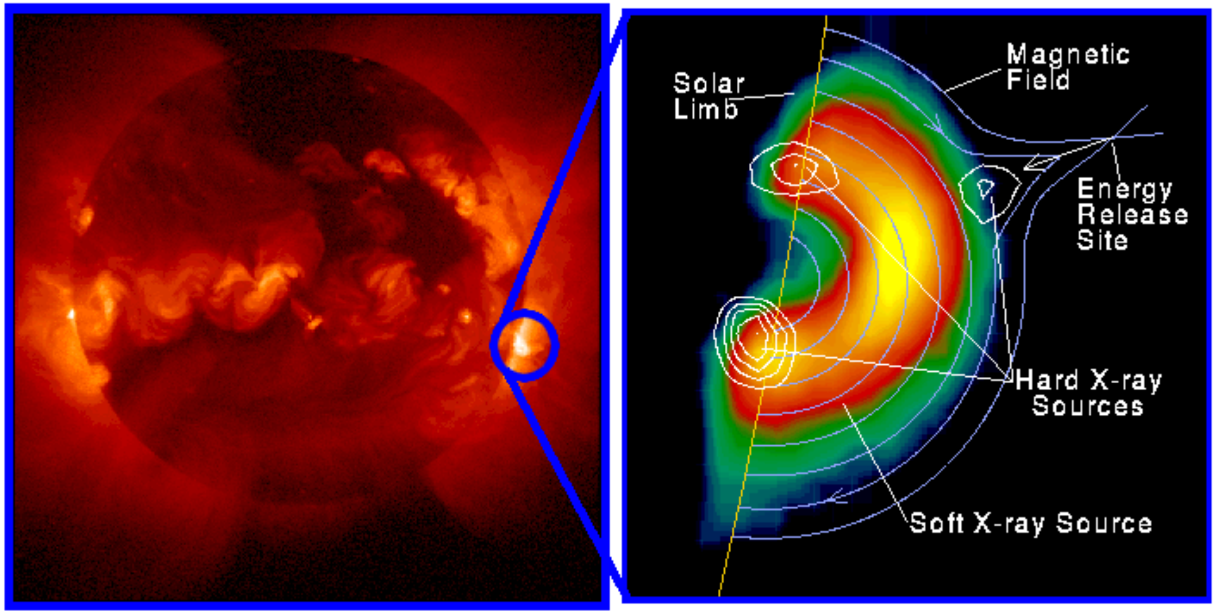

Yohkoh X-ray Image of a Solar Flare, Combined Image in Soft X-rays (left) and Soft X-rays with Hard X-ray Contours (right). Jan 13, 1992.

- Large numbers of non-thermal ions and electrons produced in flares

- Magnetic reconnection is believed to be fundamental process of energy release in solar flares

- Are direct electric fields associated with reconnection responsible for generating high energy particles?

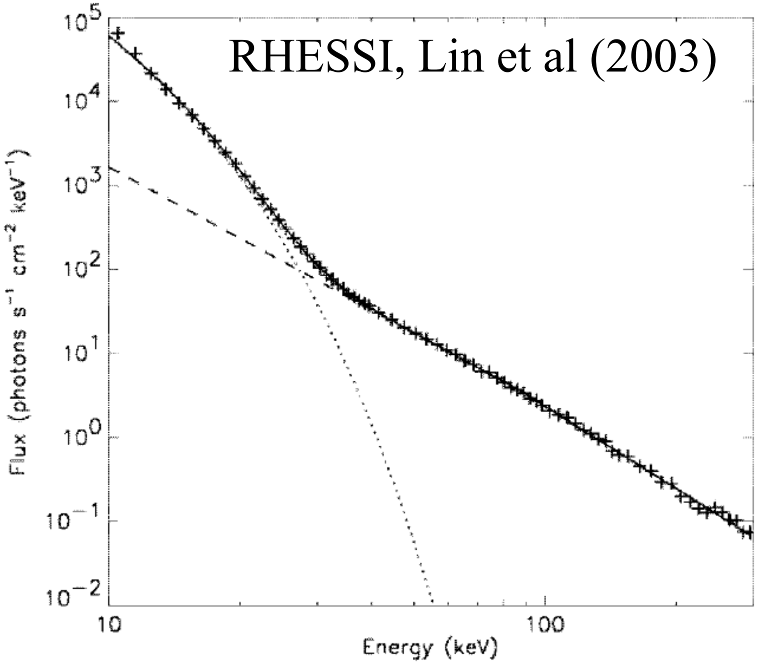
RHESSI, Lin et al (2003)

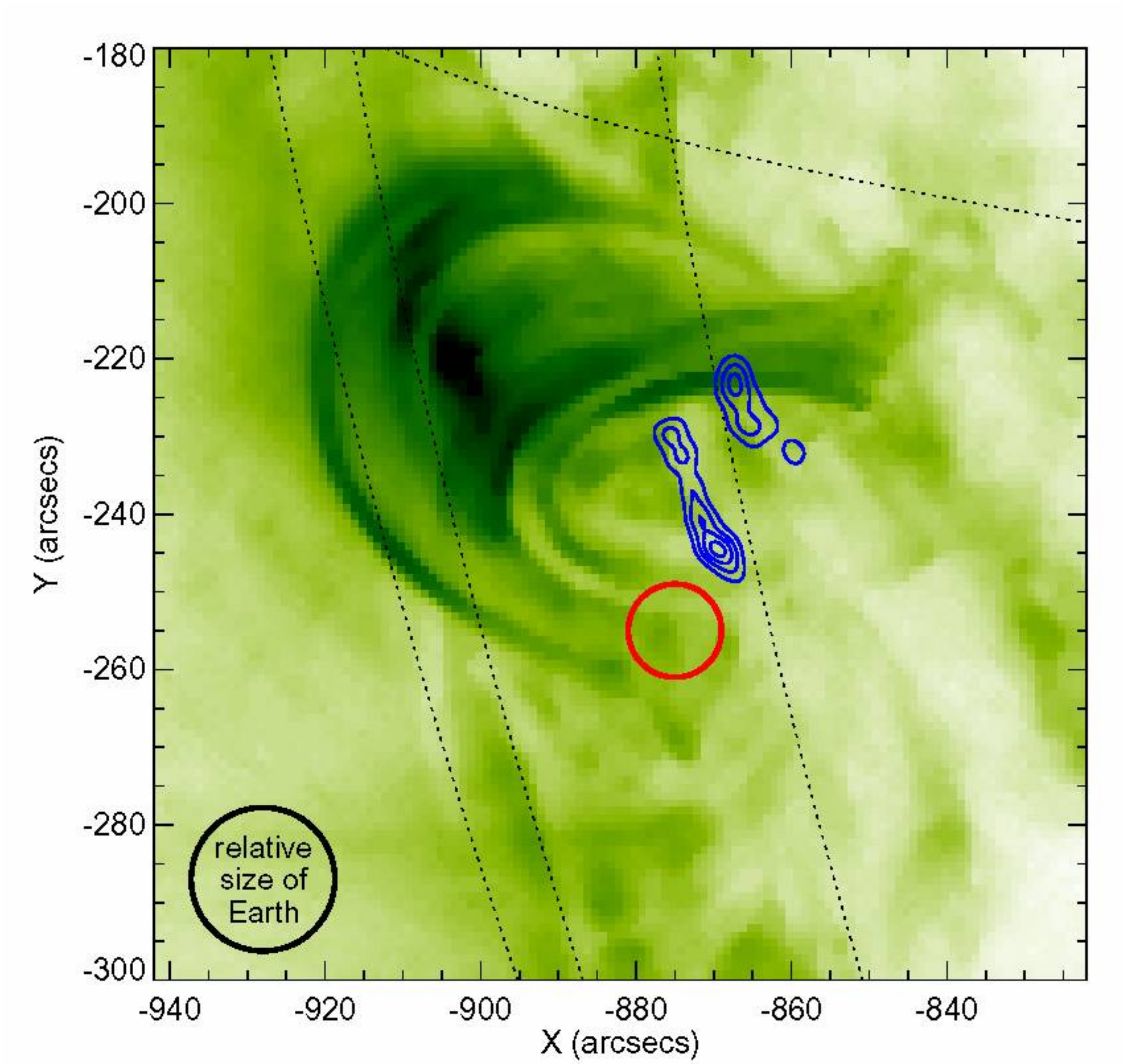

Lin et al, 2003

Magnetic field topology for TP

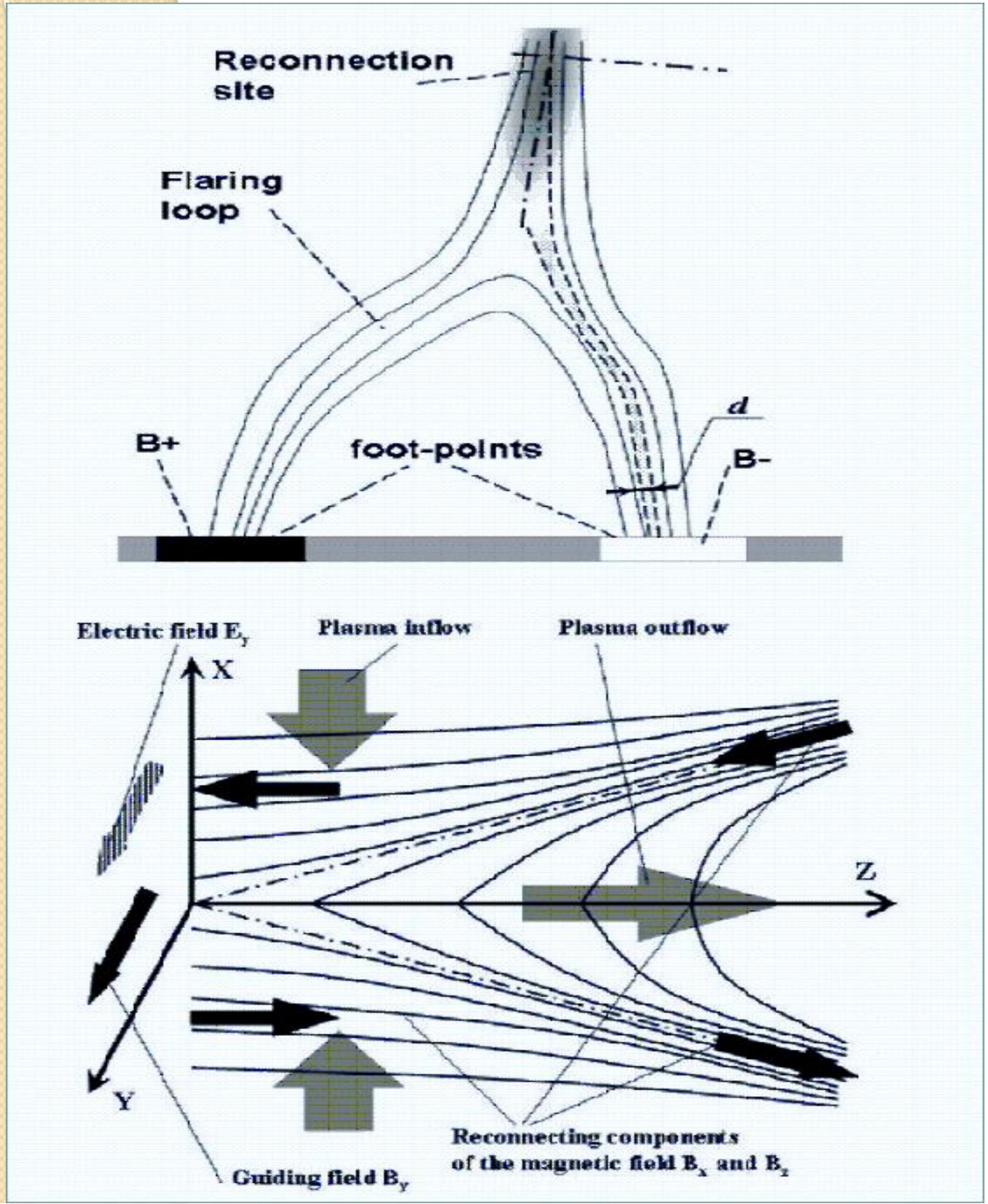

(Zharkova&Gordovskyy, ApJ, 2004, MNRAS, 2005) Sp.Sci.Rev, 2005

$B_z = B_0 \tanh(-x/d)$
$B_x = B_0 (z/a)^{\alpha}$

$B_y = +/- By_0 = 1\text{-}10$ G

$B_0 = 10\text{-}100$ G

$E_{y0} = B_0 V_{inflow} - 1/\sigma\mu\, dB_z/dx$

$V_{inflow} \approx 0.01\, V_{alfven} \approx 10^4 m/s$

⇩

$E_{y0} = 100\text{ -}250$ V/m

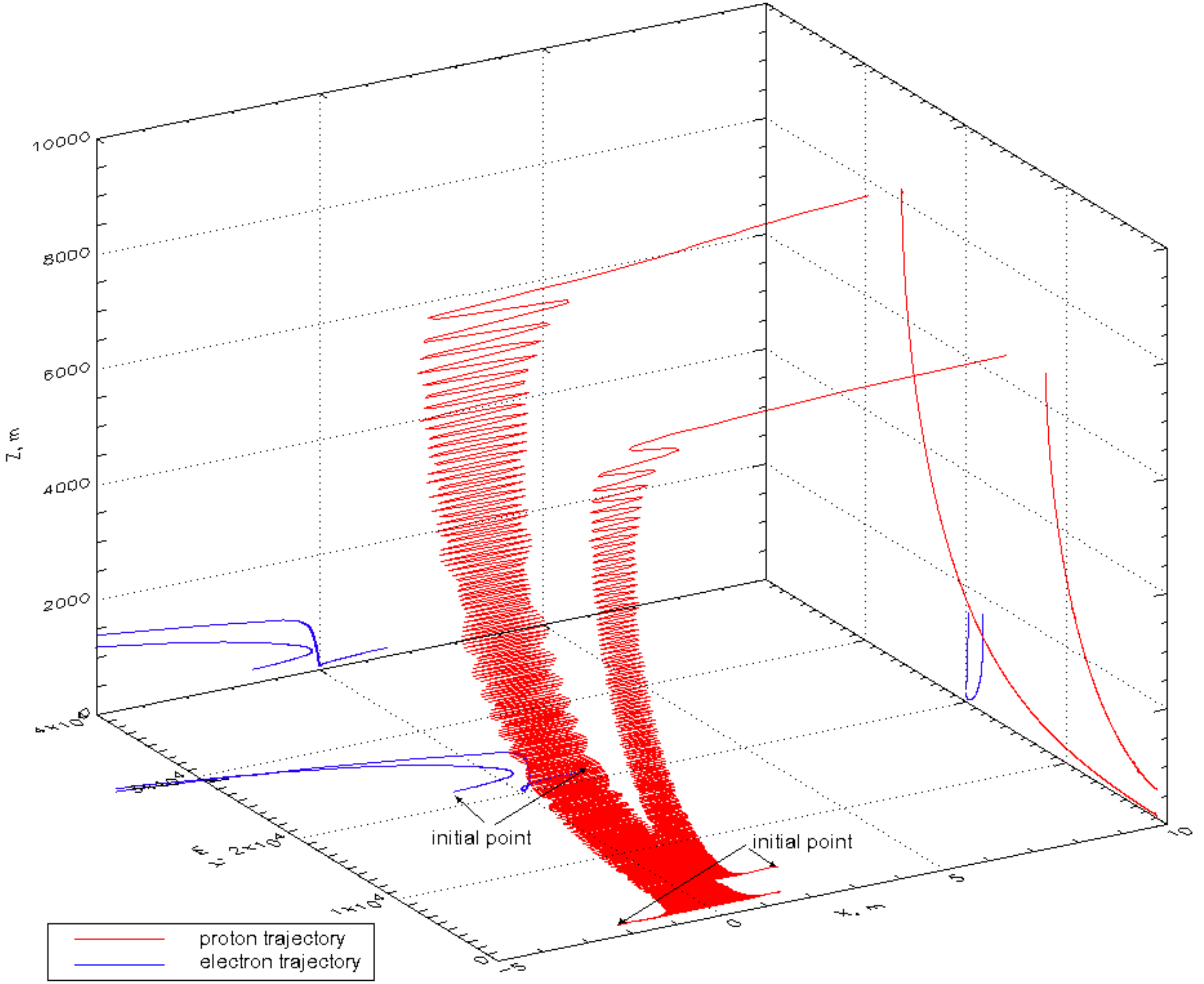

Trajectories of electrons and protons near the reconnecting current sheet plate. Protons trajectories are shown by red color and electrons trajectories are shown by blue color. For *β=0.1* the full charges separation is observed.

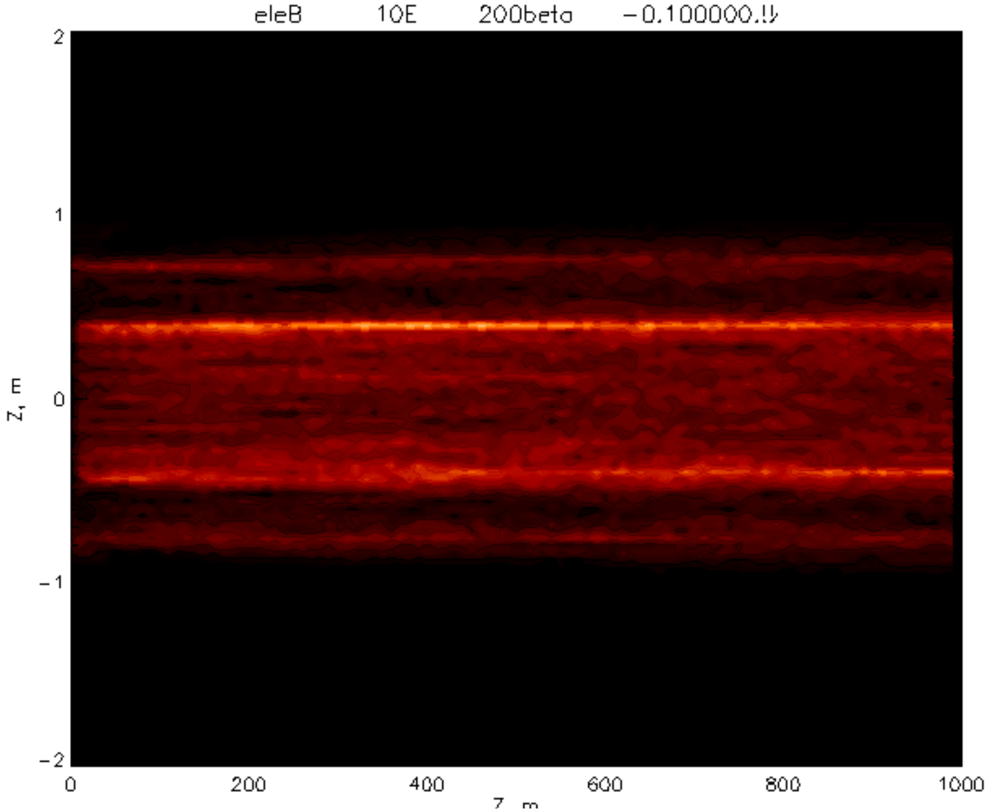

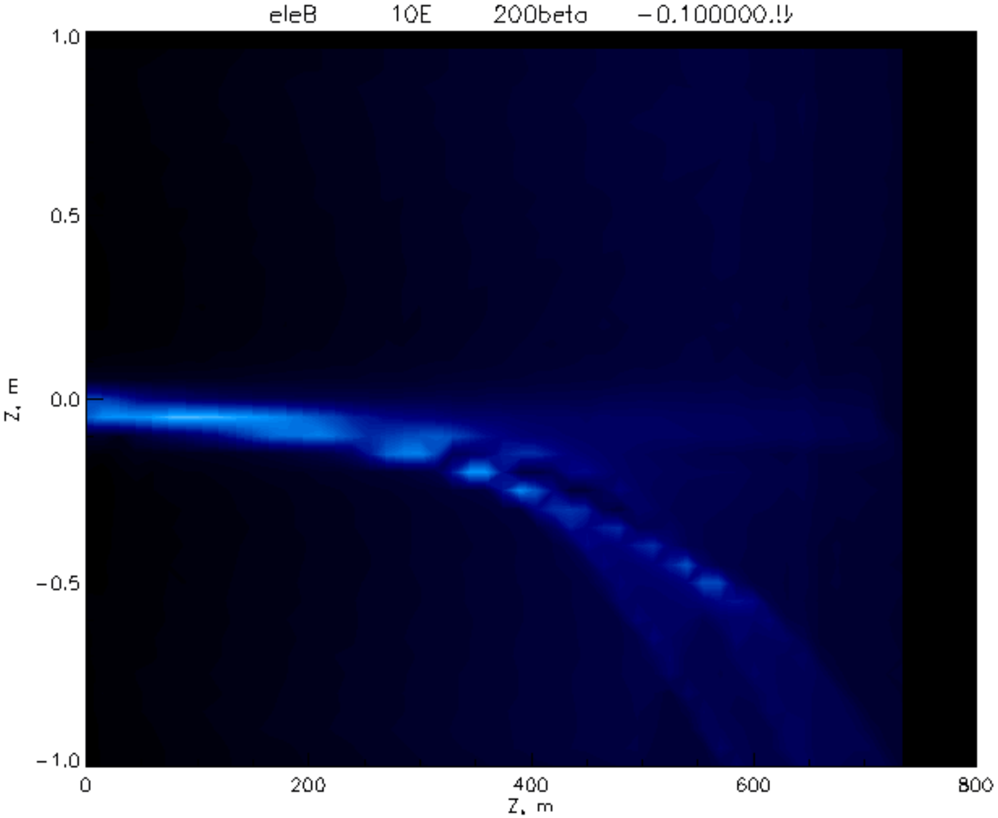

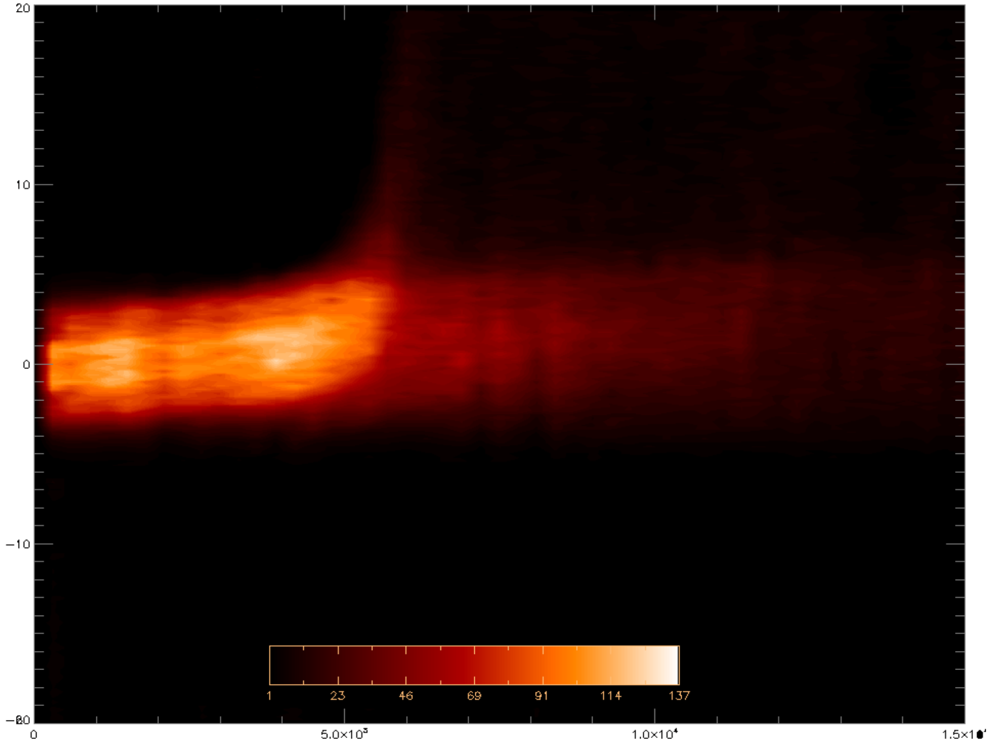

Densities of protons and electrons in an RCS.

High energy electrons (with energy about $2*10^5 – 1.2*10^6$ eV) form a particle jet ejected from the RCS. The same protons behavior is observed at a distance about $3\text{-}4x10^3$ m along Z axis

However → polarization electric field

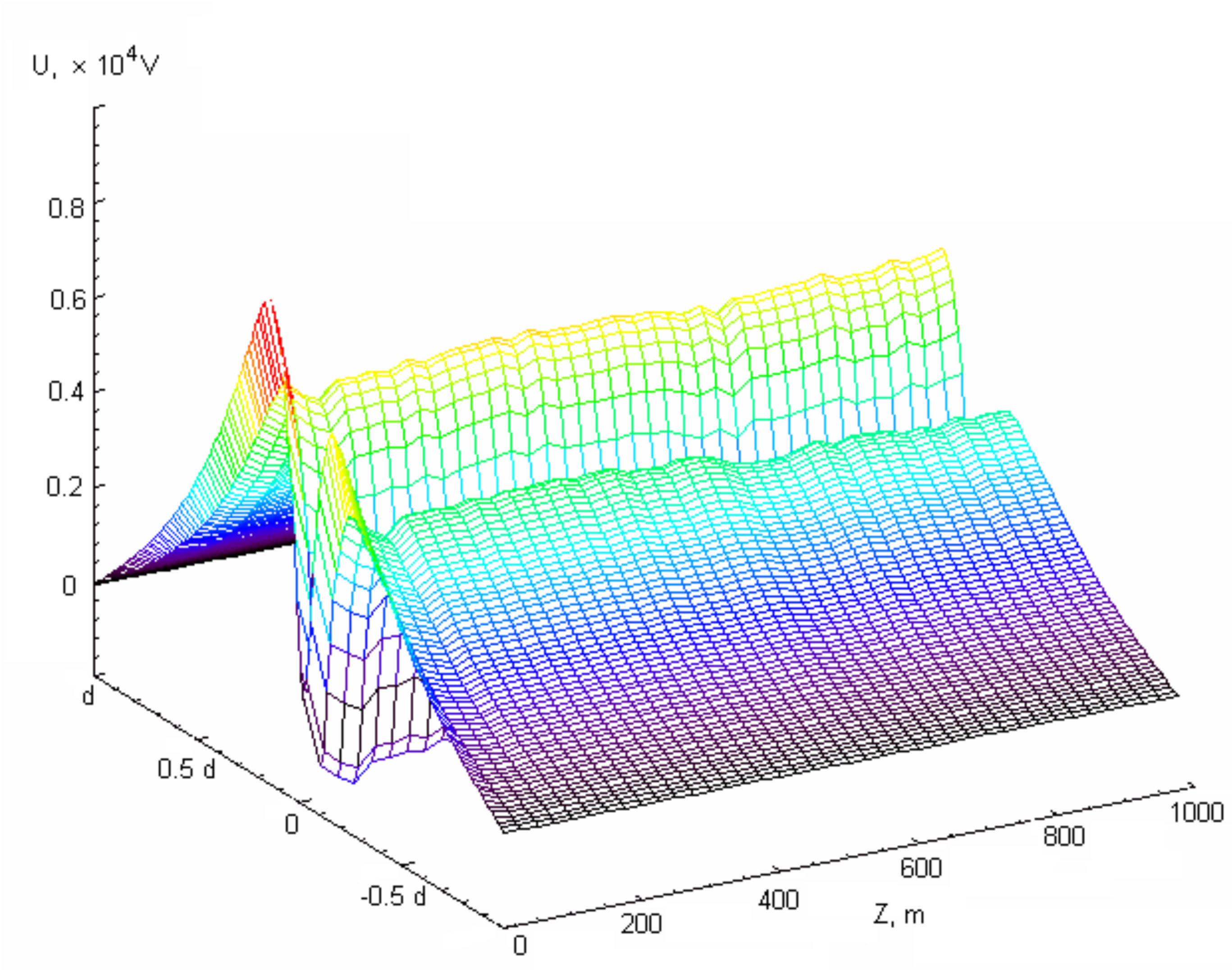

Plasma feedback in PIC simulations

(Verboncouer & Gladd, 1995, Siversky & Zharkova, 2009, JPP, Zharkova et ak, 2011)

- $\partial E/\partial t = c^2 \nabla \mathrm{x} B - 1/\varepsilon_0 \, (J_e + J_{p)}$
- $\partial B/\partial t = \nabla \mathrm{x} E$

$$\begin{aligned} \frac{d\mathbf{x}}{dt} &= \frac{\mathbf{p}}{m\gamma} \\ \frac{d\mathbf{p}}{dt} &= q\left(\mathbf{E} + \frac{1}{c}\frac{\mathbf{p}}{m\gamma} \times \mathbf{B}\right) \end{aligned}$$

$$d_e \equiv L^{-1}\left(c/\omega_{pe}\right)$$

Electron’s skin depth

$$d_i \equiv L^{-1}\left(c/\omega_{pi}\right)$$

Ion’s skin depth

PIC – low density

$$n = 10^4 \mathrm{cm}^{-3}$$

$$B_0 = 100\mathrm{G} \qquad B_y = 1\mathrm{G}$$

$$B_x = 0.4\mathrm{G} \qquad \frac{m_p}{m_e} = 10$$

x-V_z phase space

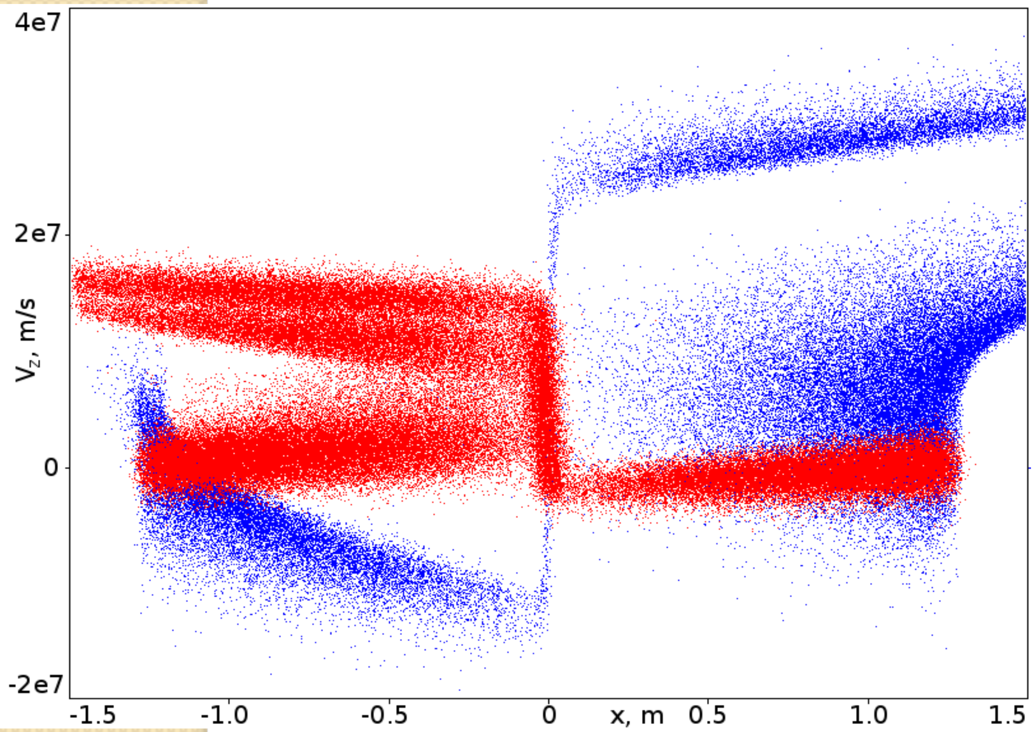

Energy distribution of ejected particles

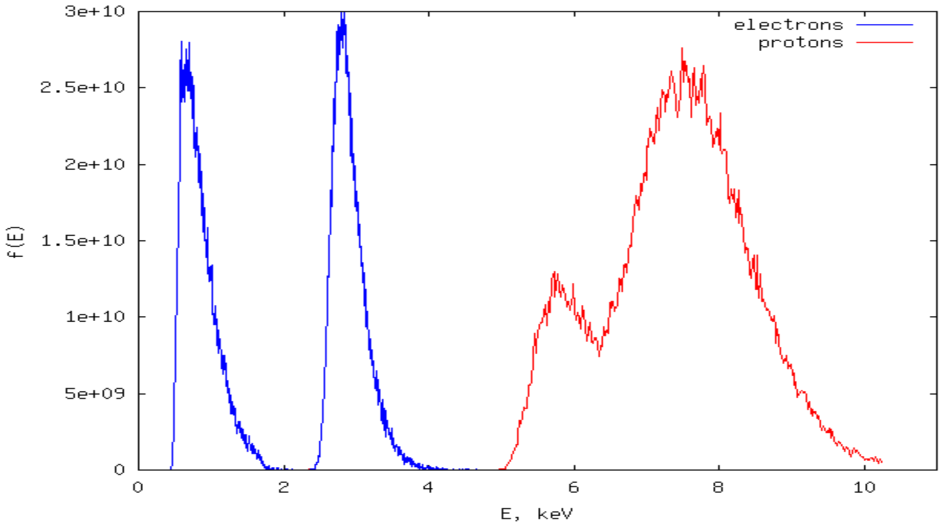

Pitch angle distribution of ejected particles

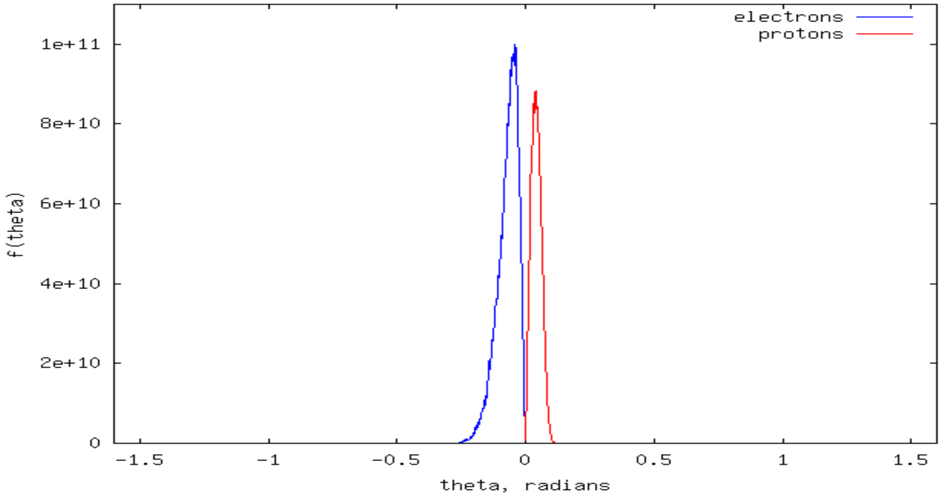

PIC – higher density

$$B_0 = 10\text{G} \qquad B_y = 1\text{G}$$

$$B_x = 0.4\text{G} \qquad \frac{m_p}{m_e} = 10$$

x-V_z phase space

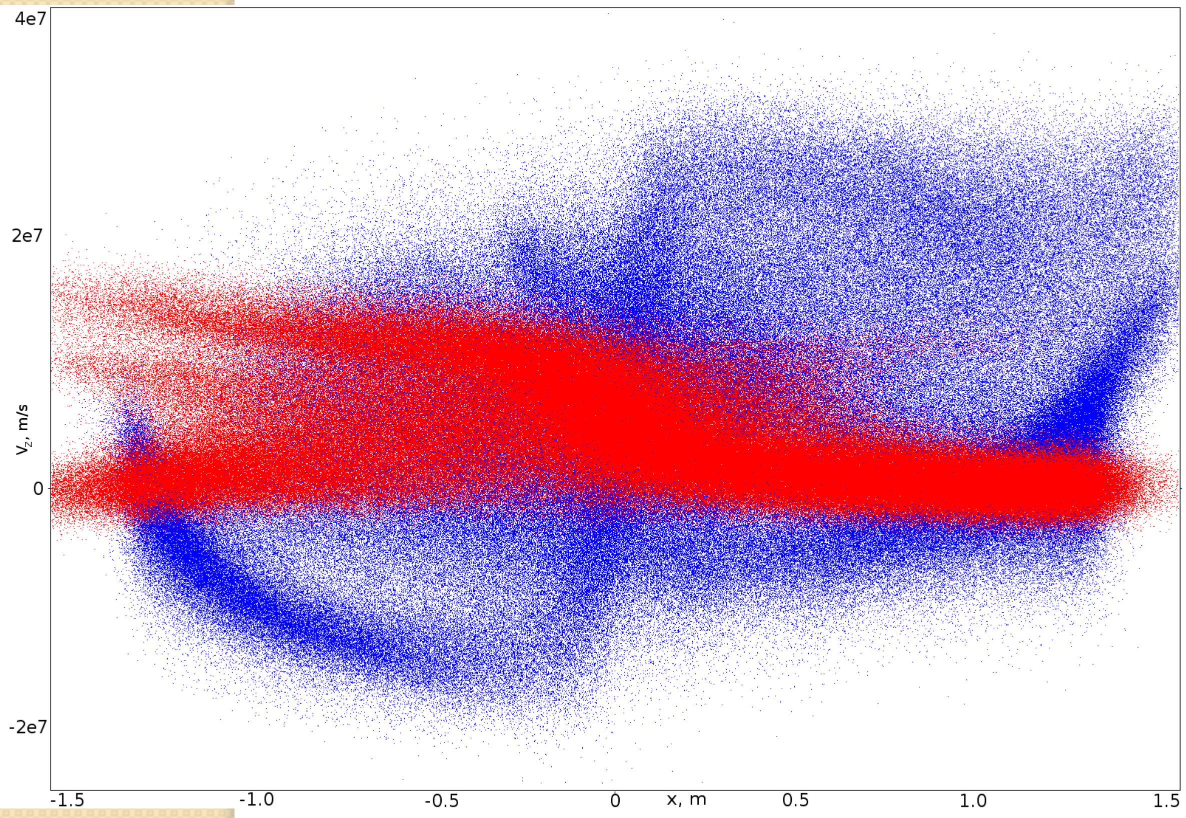

$$n = 10^6\text{cm}^{-3}$$

Energy distributions

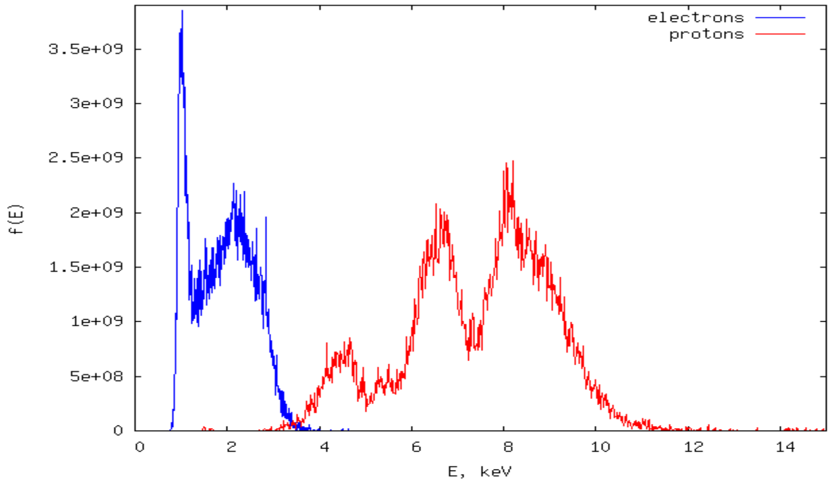

Pitch angle distributions

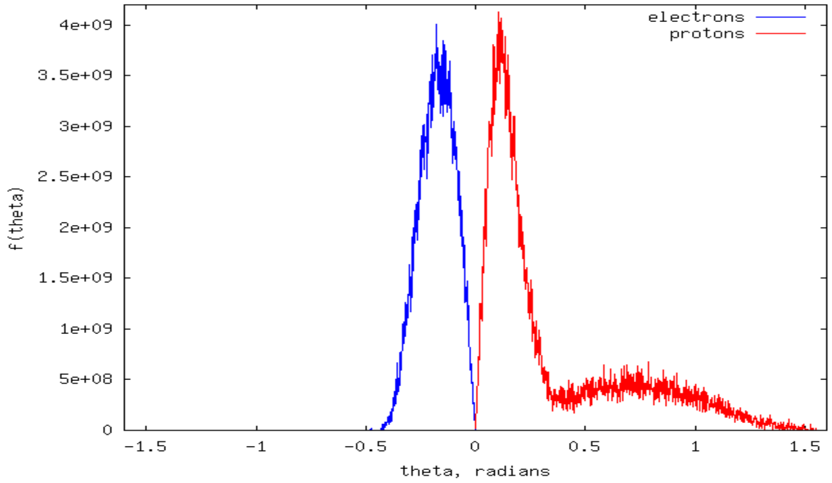

Energy spectra

PIC – low density

red – test particle
blue – PIC simulation

$$\frac{dN}{d\varepsilon} \propto n_0 \left(\frac{d\varepsilon}{dB_x} \frac{dB_x}{dz} \right)^{-1}$$

where

$$B_x(z) = B_0 \frac{z}{a}$$

upper – protons
lower – electrons

B_0 = 100 G

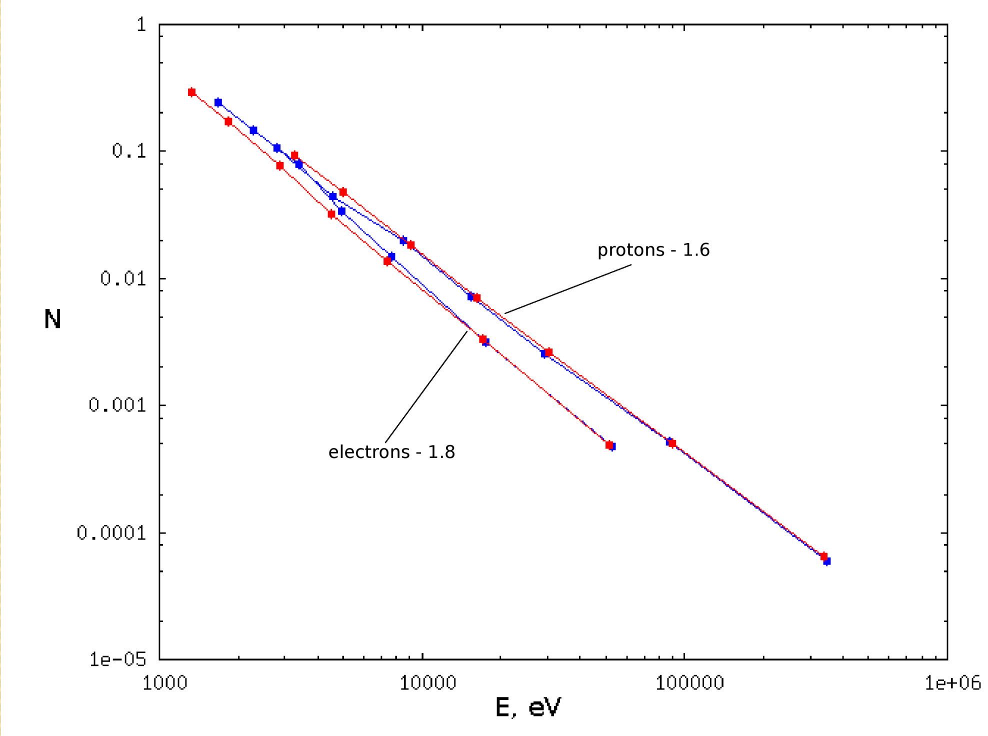

B_0 = 10 G

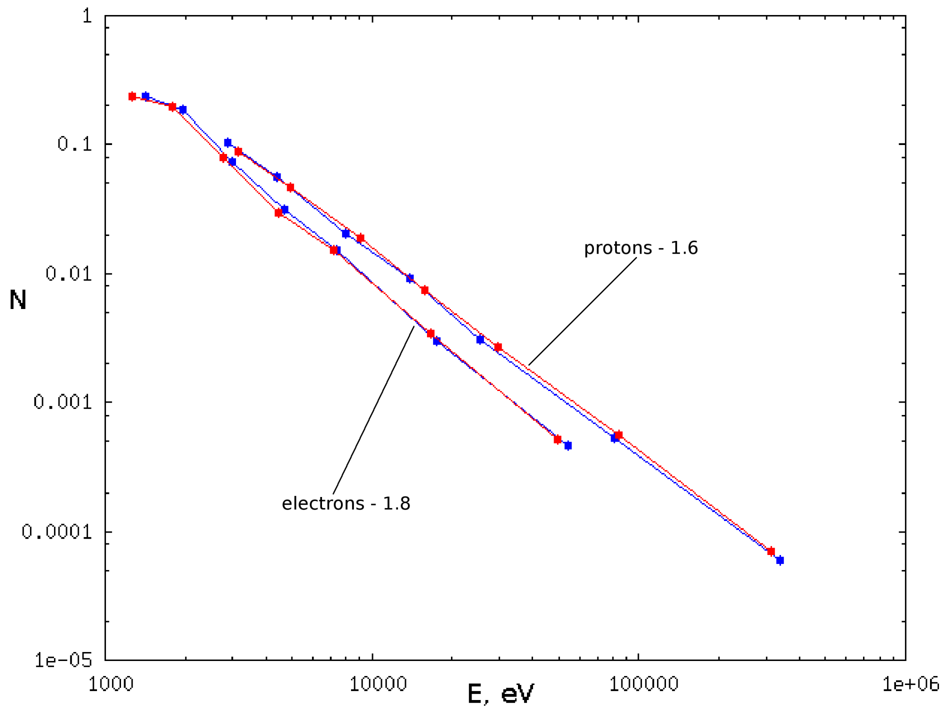

Polarization electric field

Siversky & Zharkova, 2009, JPP

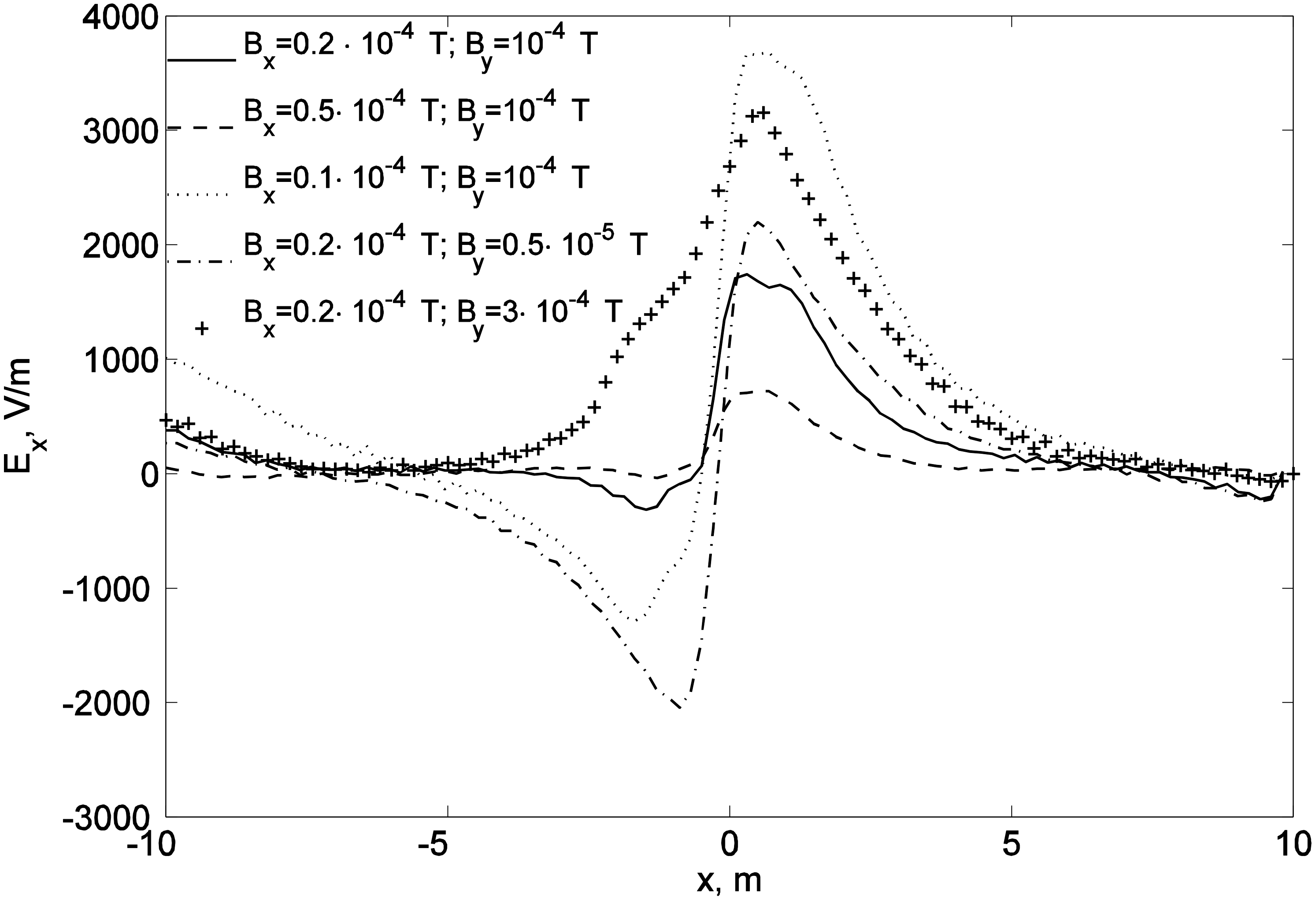

PIC – Langmuir waves

Induced electric field E_z

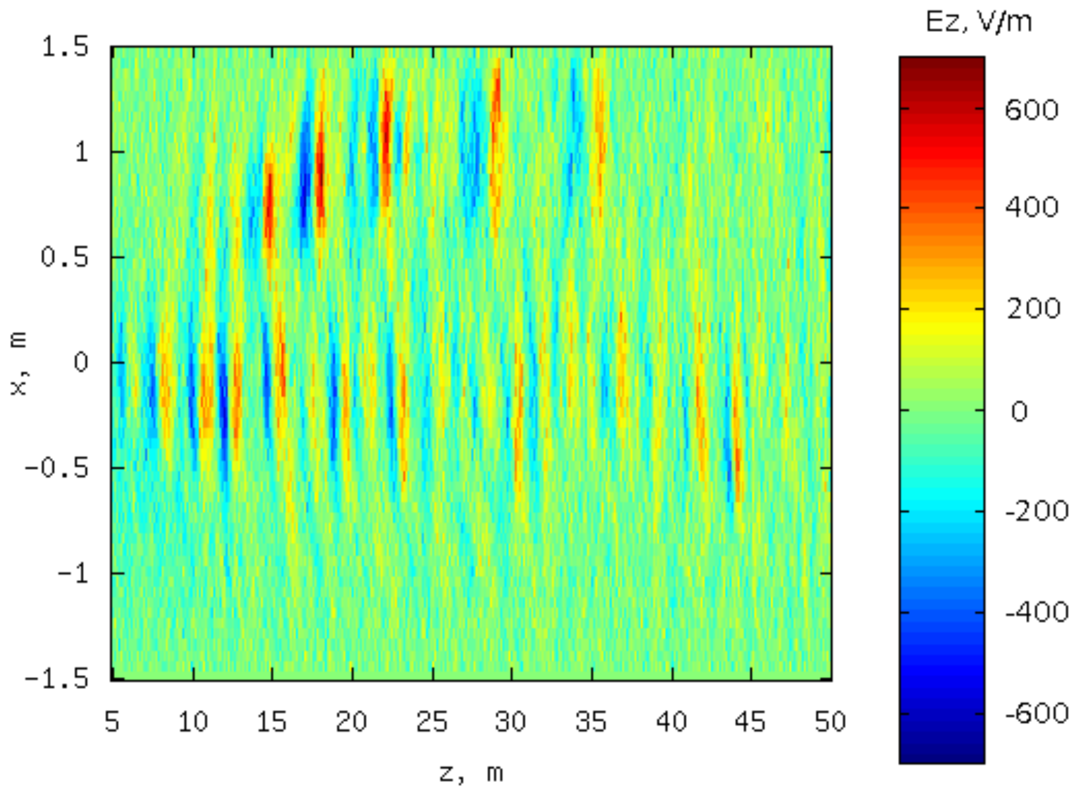

→ Langmuir wave

$$\lambda \sim 2\mathrm{m}$$

$$T \sim 2 \cdot 10^{-7}\mathrm{s}$$

$$V_{ph} \sim 10^{7}\mathrm{m/s}$$

$$\gamma \sim 5 \cdot 10^{6}\mathrm{s}^{-1}$$

HXR observations and (steady) thick target model

- What do we really observe in HXR light curves since the era of SMM?

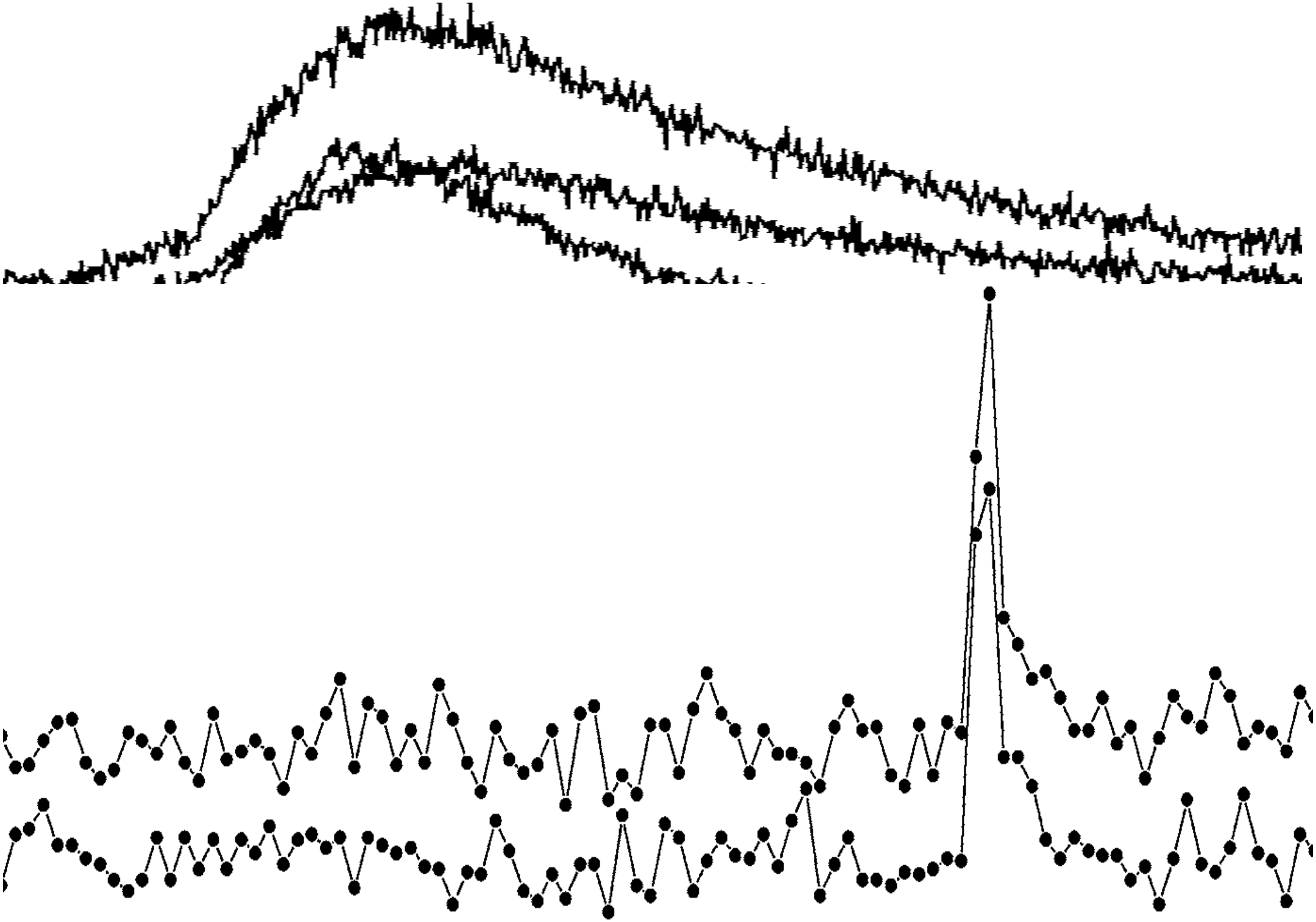

PARTICLE PRECIPITATION

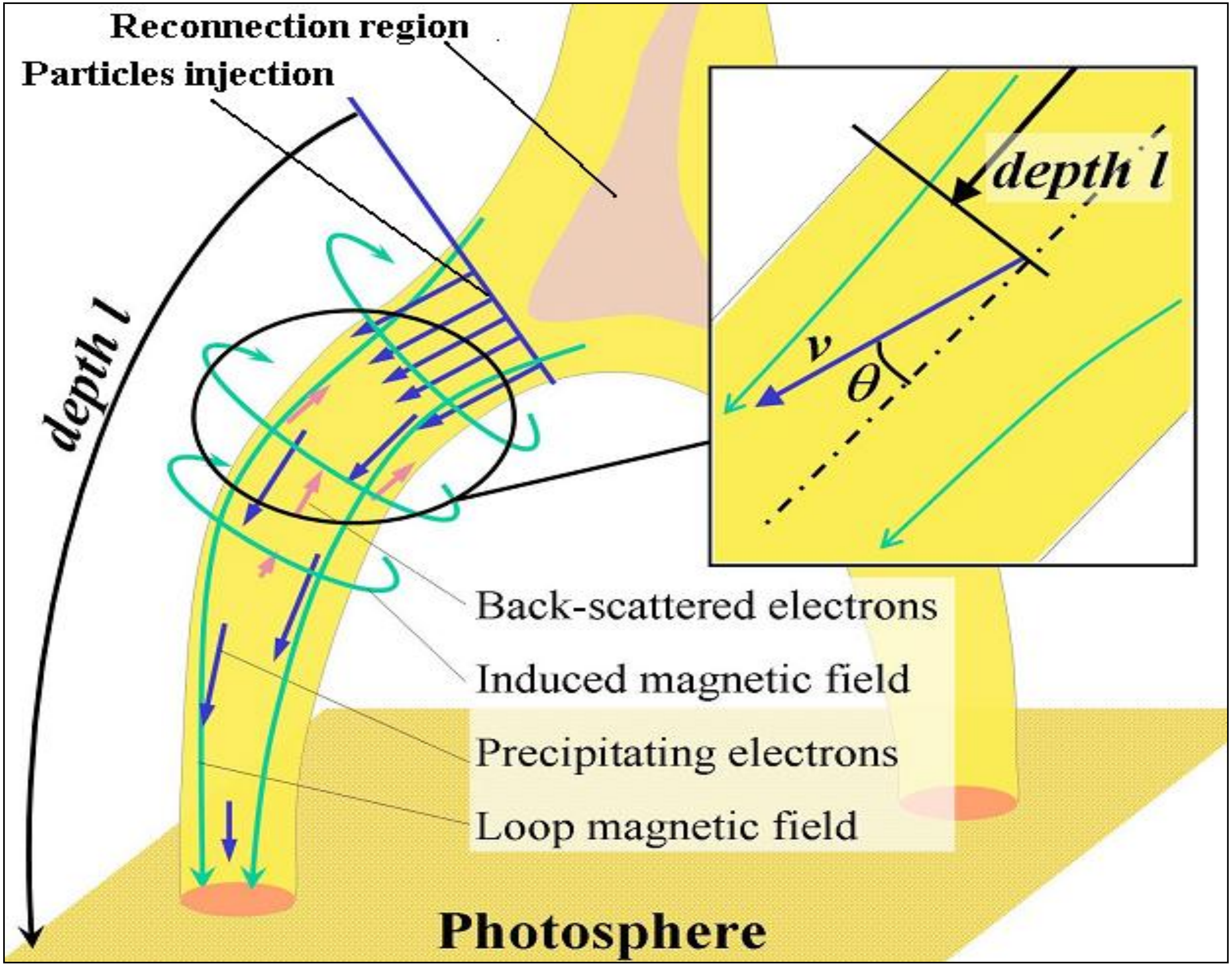

Particle scattering in Coulomb collisions

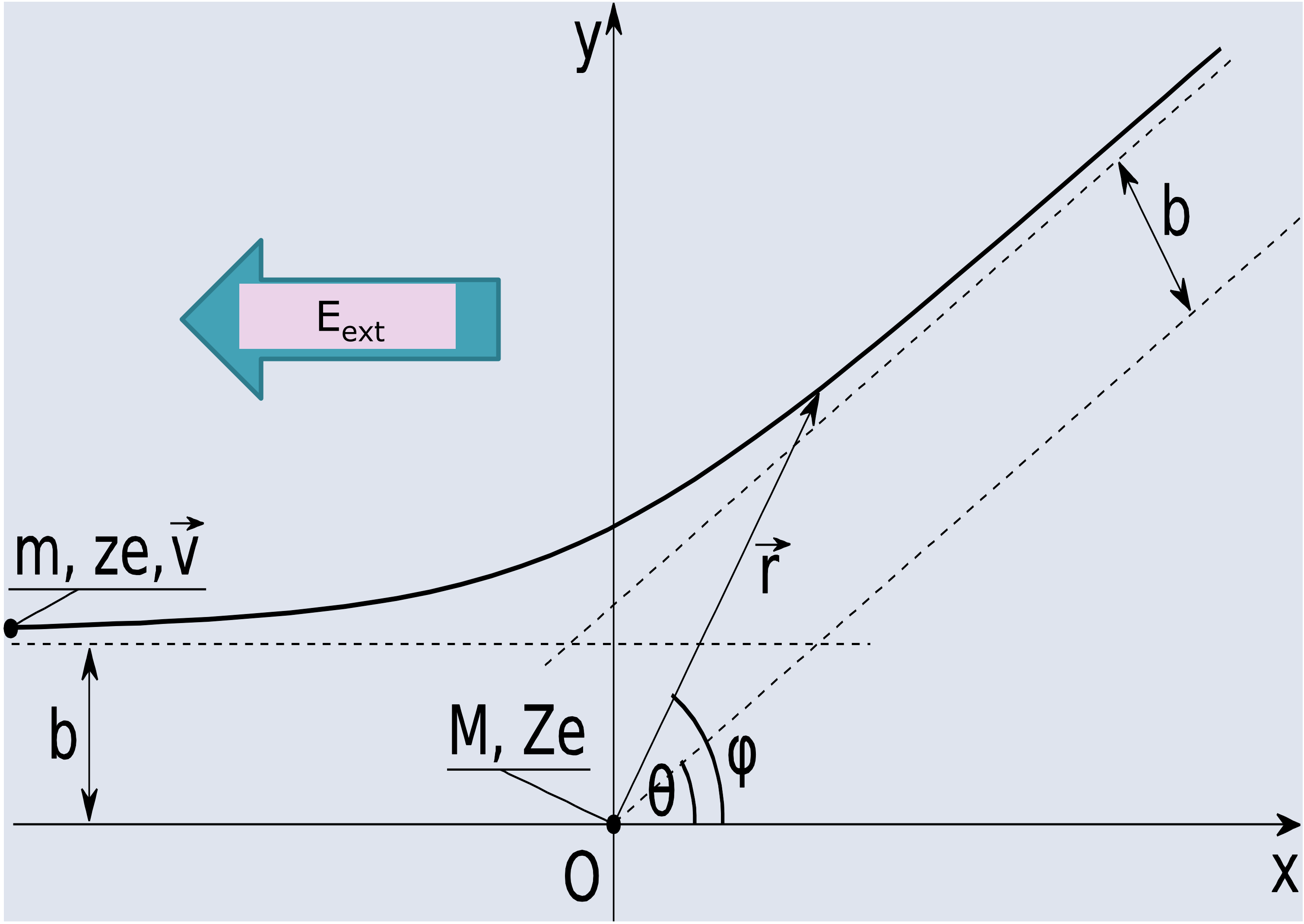

RHESSI 2010

Fokker-Planck equation

$$f = f(t, s, E, \mu)$$

t – time
s – column depth
E – energy
μ – pitch angle cosine

self-induced (return current) electric field

$$\frac{\partial f}{\partial t} + n\sqrt{E}\mu\frac{\partial f}{\partial s} - 2\mathcal{E}\mu\sqrt{E}\frac{\partial f}{\partial E} - \mathcal{E}\frac{1-\mu^2}{\sqrt{E}}\frac{\partial f}{\partial \mu} =$$

$$n\frac{1}{\sqrt{E}}\frac{\partial f}{\partial E} + n\frac{1}{2E^{3/2}}\frac{\partial}{\partial \mu}\left(\left(1-\mu^2\right)\frac{\partial f}{\partial \mu}\right) - n\frac{\left(1-\mu^2\right)\sqrt{E}}{2}\frac{\partial \ln B}{\partial s}\frac{\partial f}{\partial \mu}$$

collisions with ambient plasma

converging magnetic field

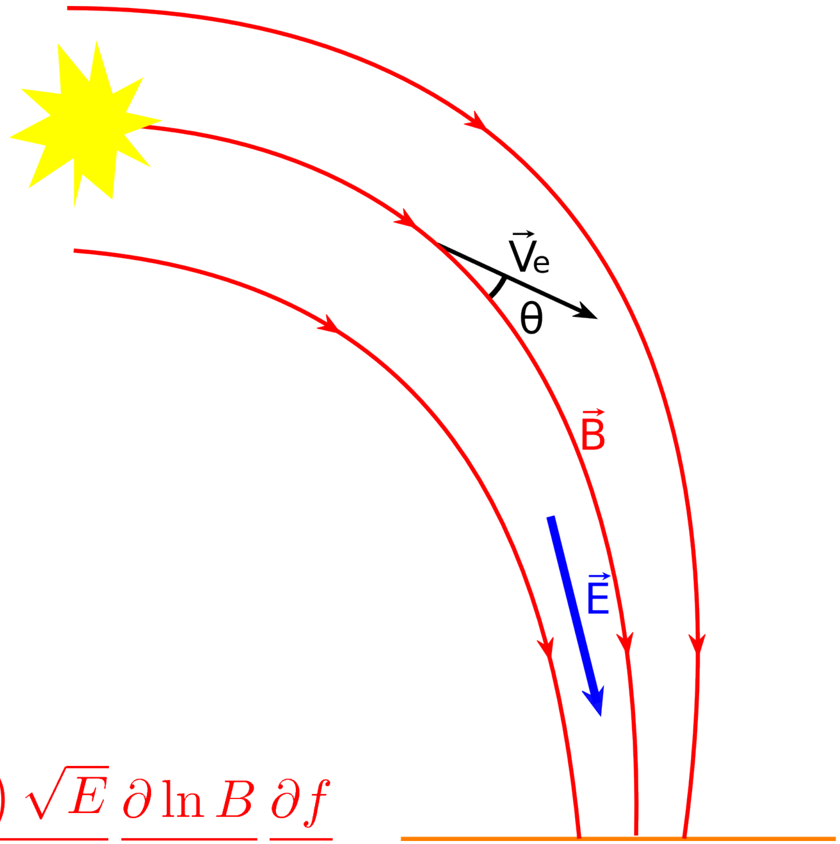

n(*s*) and *T*(*s*) are taken from the hydro-dynamic model (Zharkova, V. & Zharkov, S., ApJ, 664, 573, 2007)

Impulsive injection

$F_0 = 10^{10}$ erg cm^{-2} s^{-1}. Power law index is 3. Impulse length is $1.7 \cdot 10^{-3}$s.
Only collisions are taken into account.

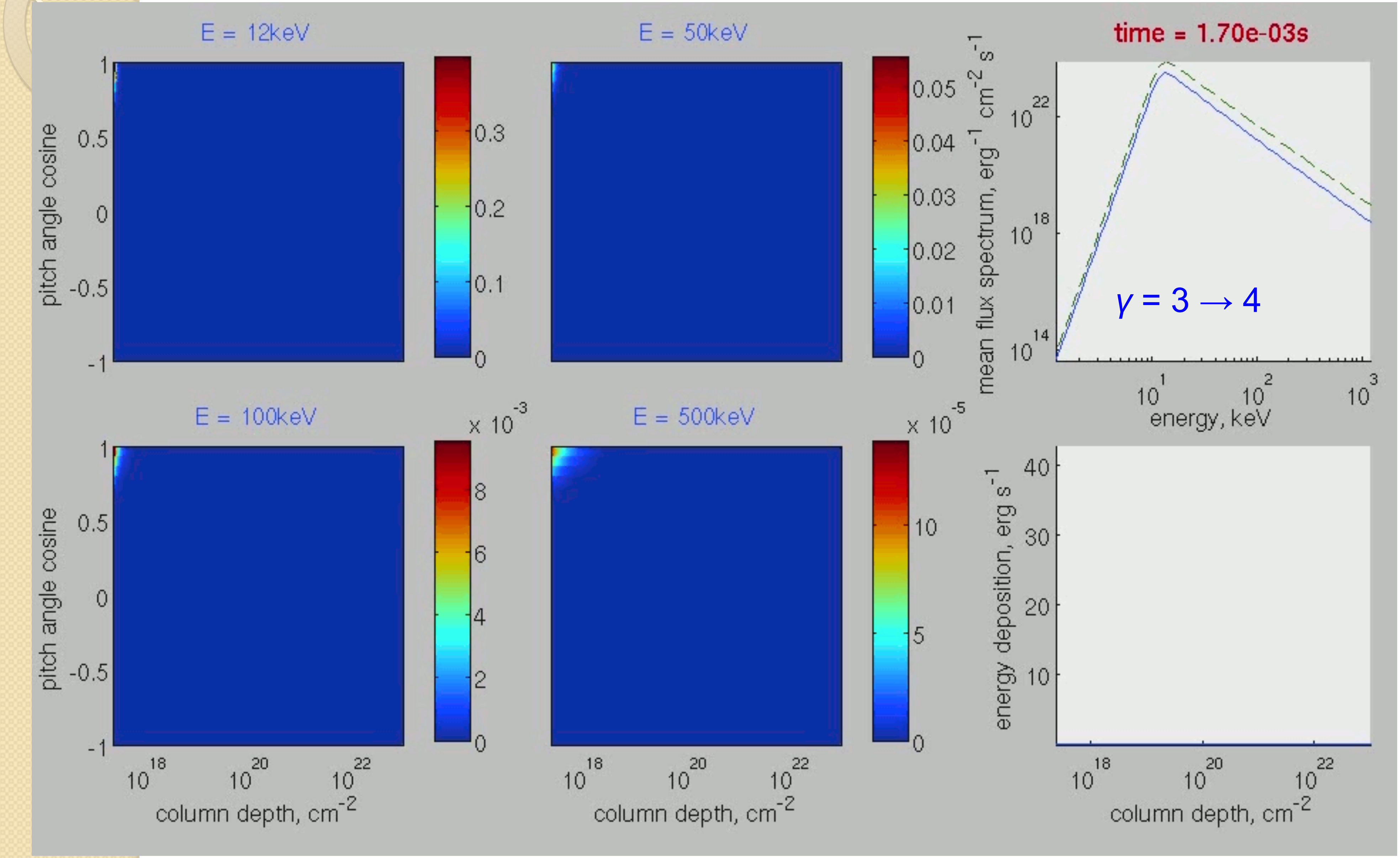
$\gamma = 3 \rightarrow 4$

Impulsive injection

$F_0 = 10^{10}$ erg cm^{-2} s^{-1}. Power law index = 3.
Collisions and magnetic convergence are taken into account.

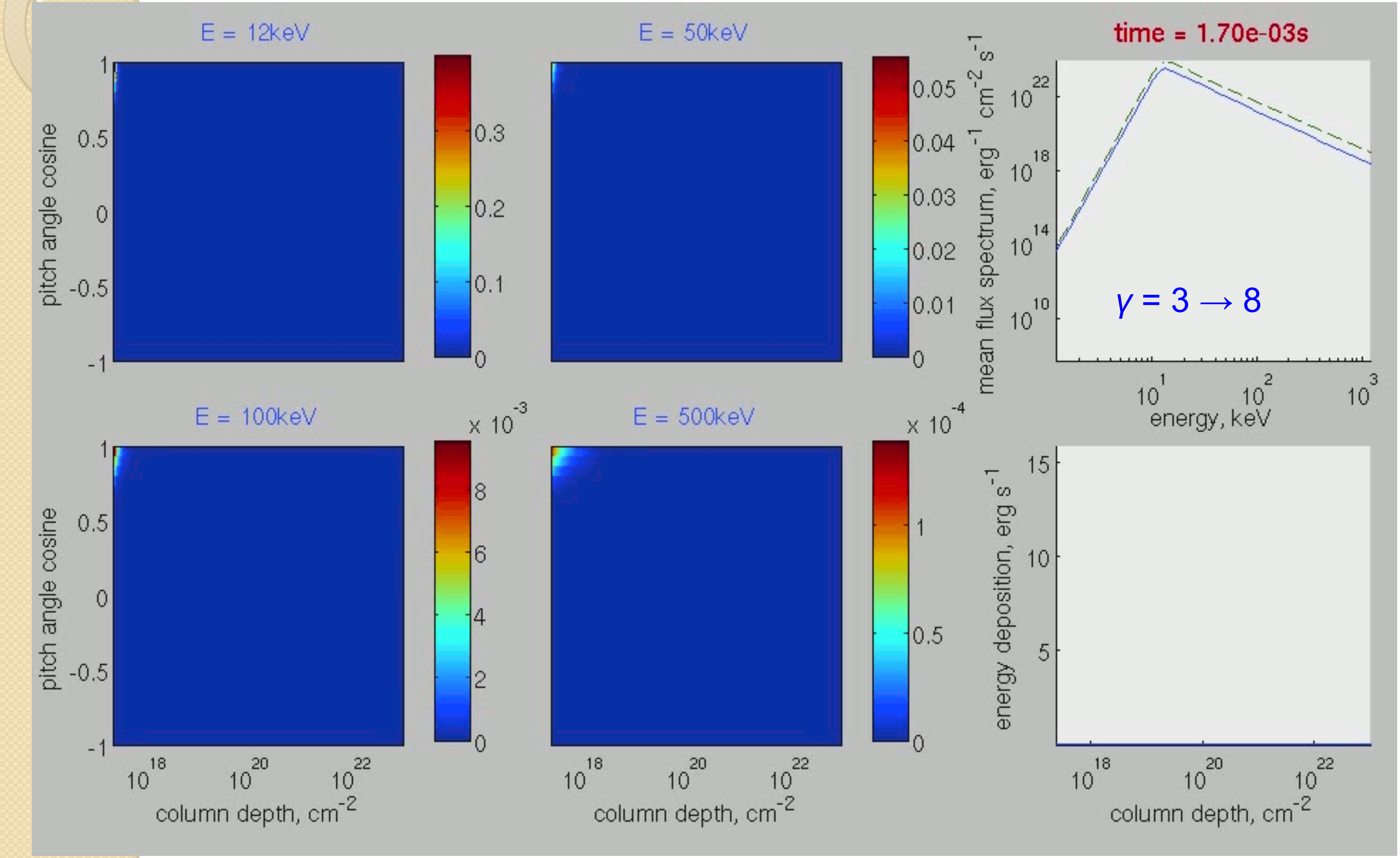

Impulse intensity variations in space and time (Siversky&Zharkova, A&A, 2009)

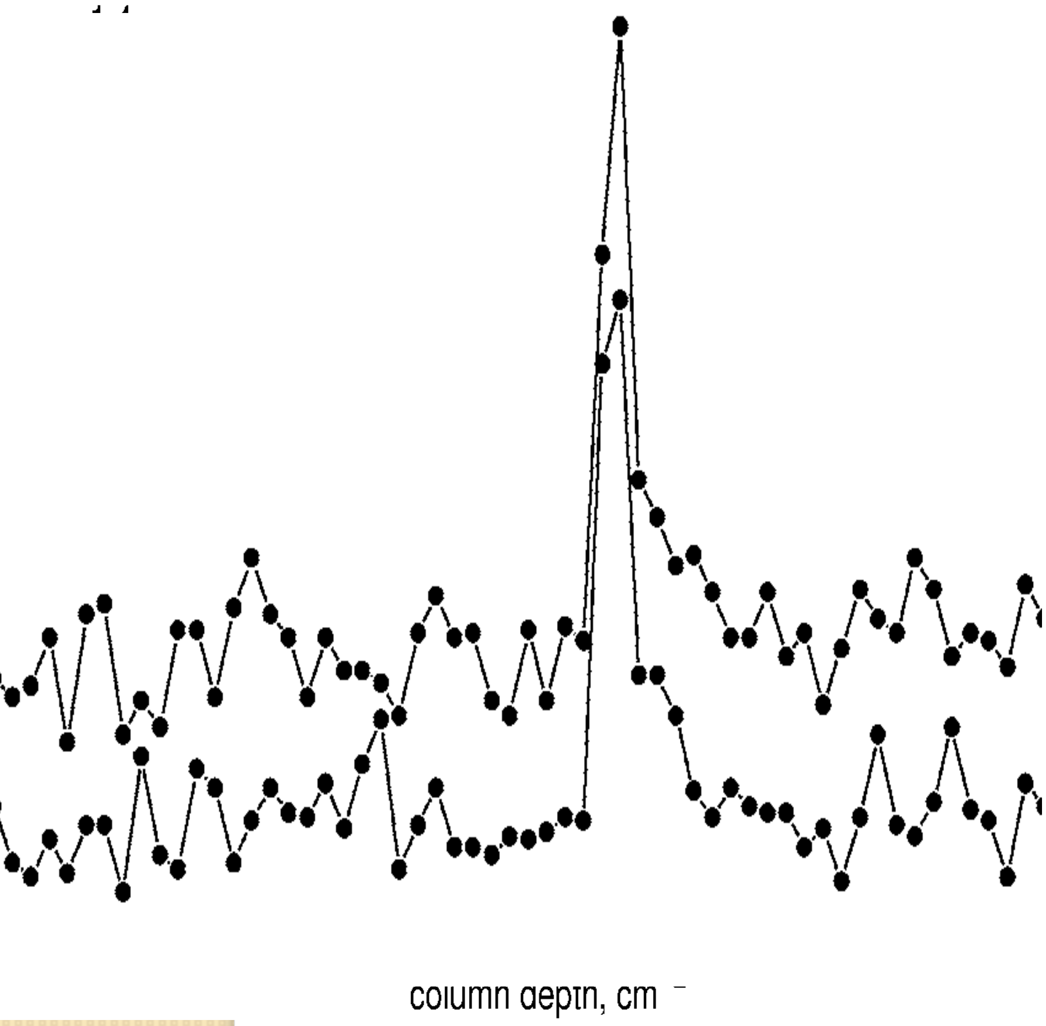

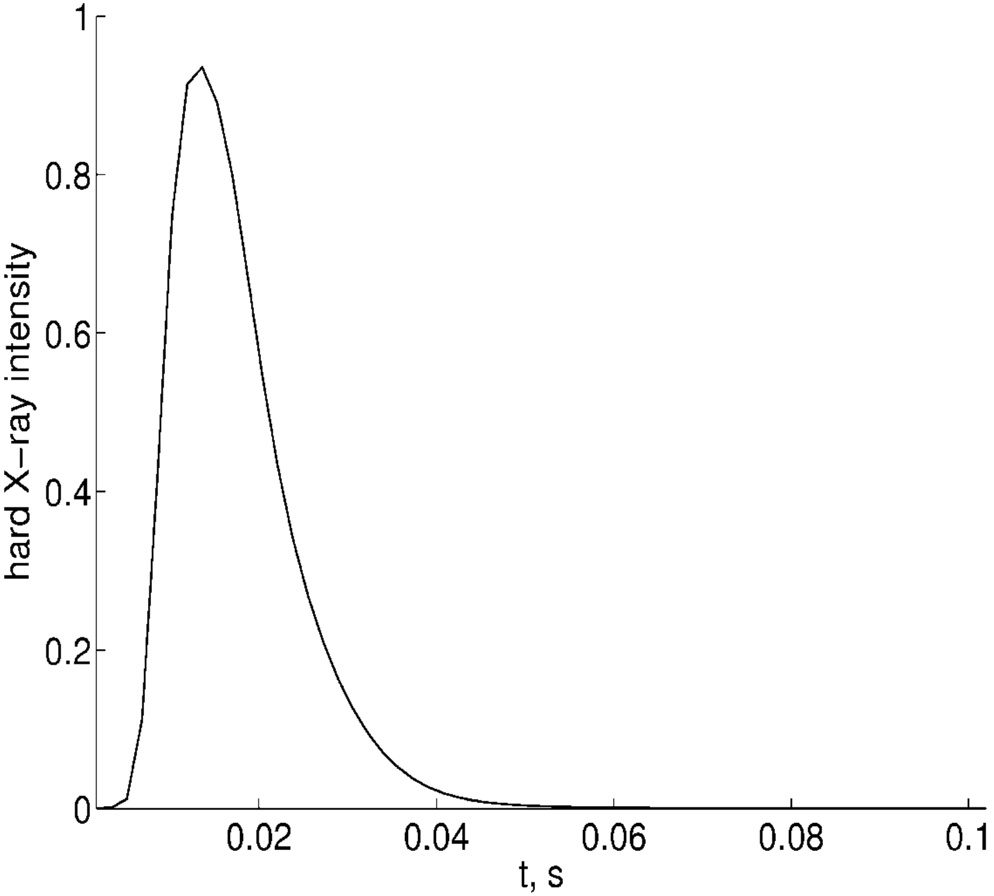

Stationary injection

Distribution function of the injected beam

$$f\left(t, s = s_{min}, z, \mu > 0\right) = f_n \psi\left(t\right) \frac{E^{\delta-1}}{E^{\delta+\gamma} + E_0^{\delta+\gamma}} \exp\left(-\frac{\left(1-\mu\right)^2}{\Delta\mu^2}\right)$$

Initial power law index of high energy electrons $\gamma = 3$
Initial pitch angle dispersion $\Delta\mu = 0.2$
Lower energy cut-off $E_0 = 12$ keV
Energy flux on the top boundary is $F_0 = 10^{10}$ erg cm^{-2} s^{-1}

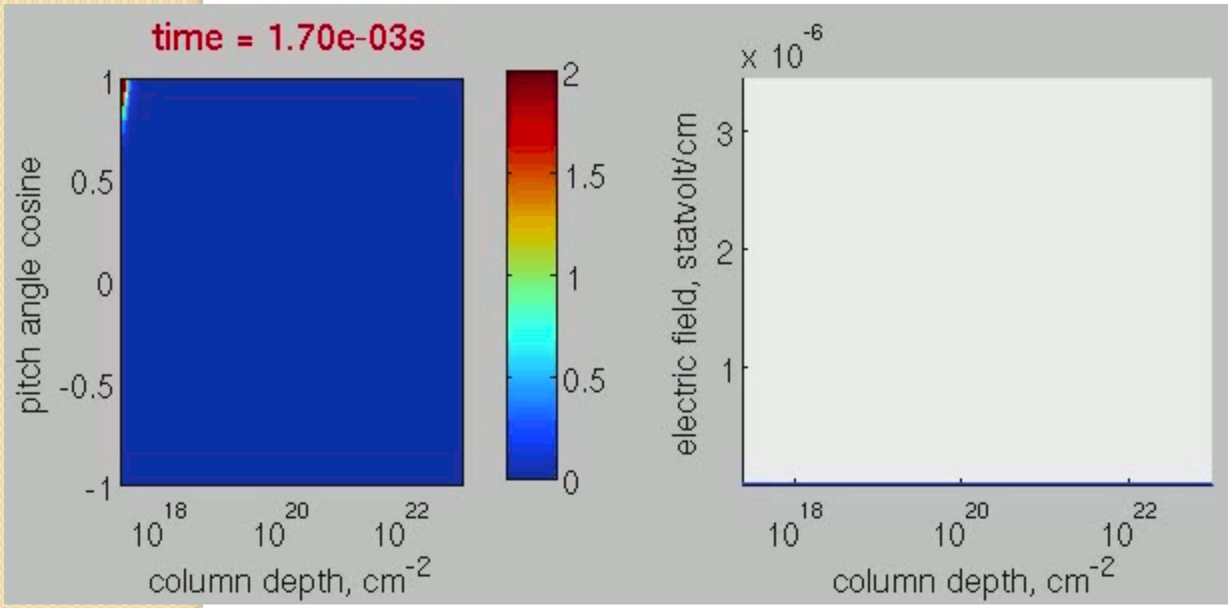

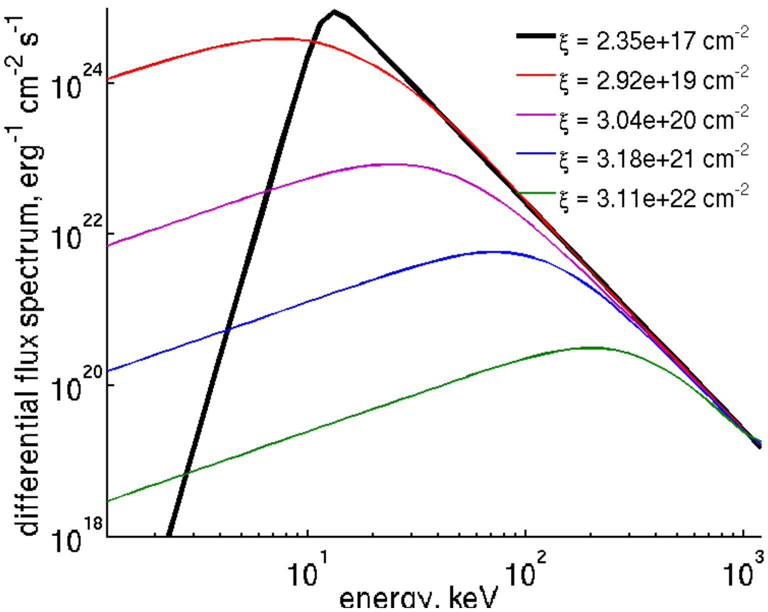

Relaxation time is ≈ 0.07s (depends mostly on density profile)

Relaxation to steady state – 0.07-0.2 s beam density N and induced E

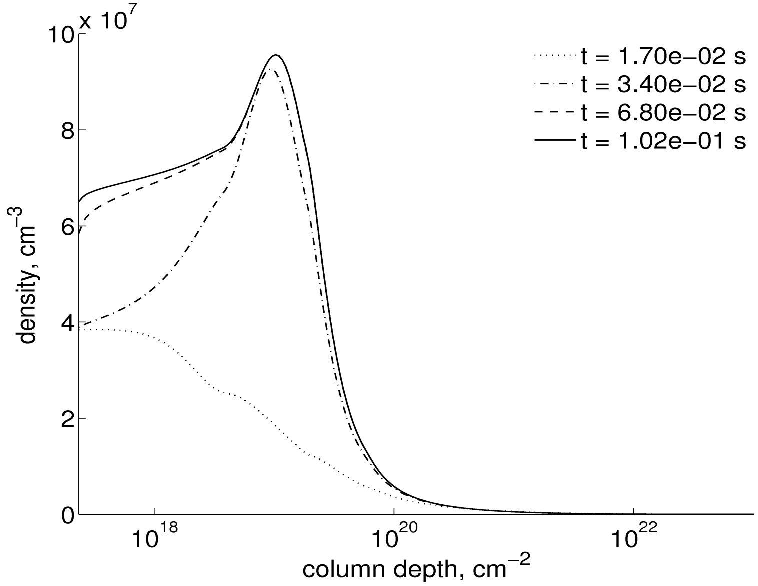

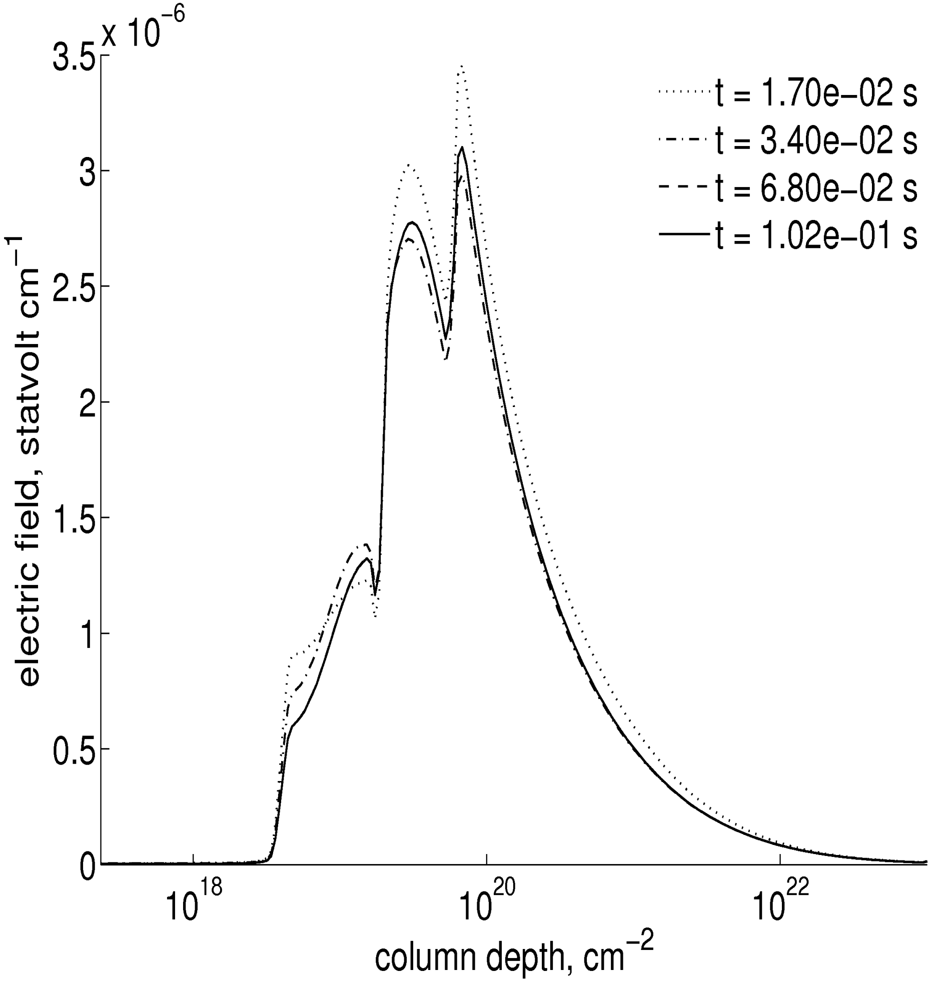

Pitch angle effects for different models

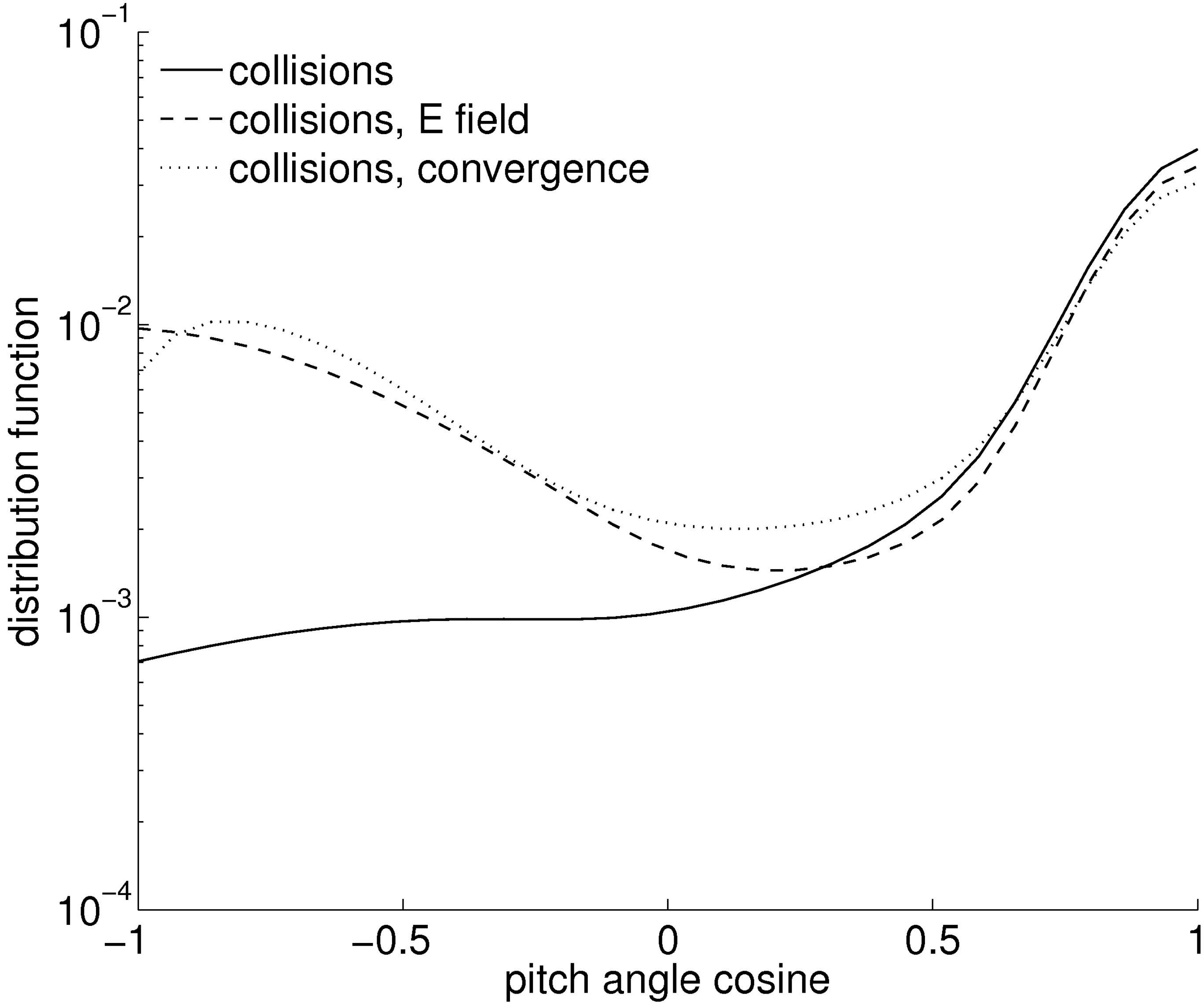

Electron distribution functions (quasi-stationary state)

at $\xi=10^{18}$ cm^{-2} (Zharkova etal, 2010)

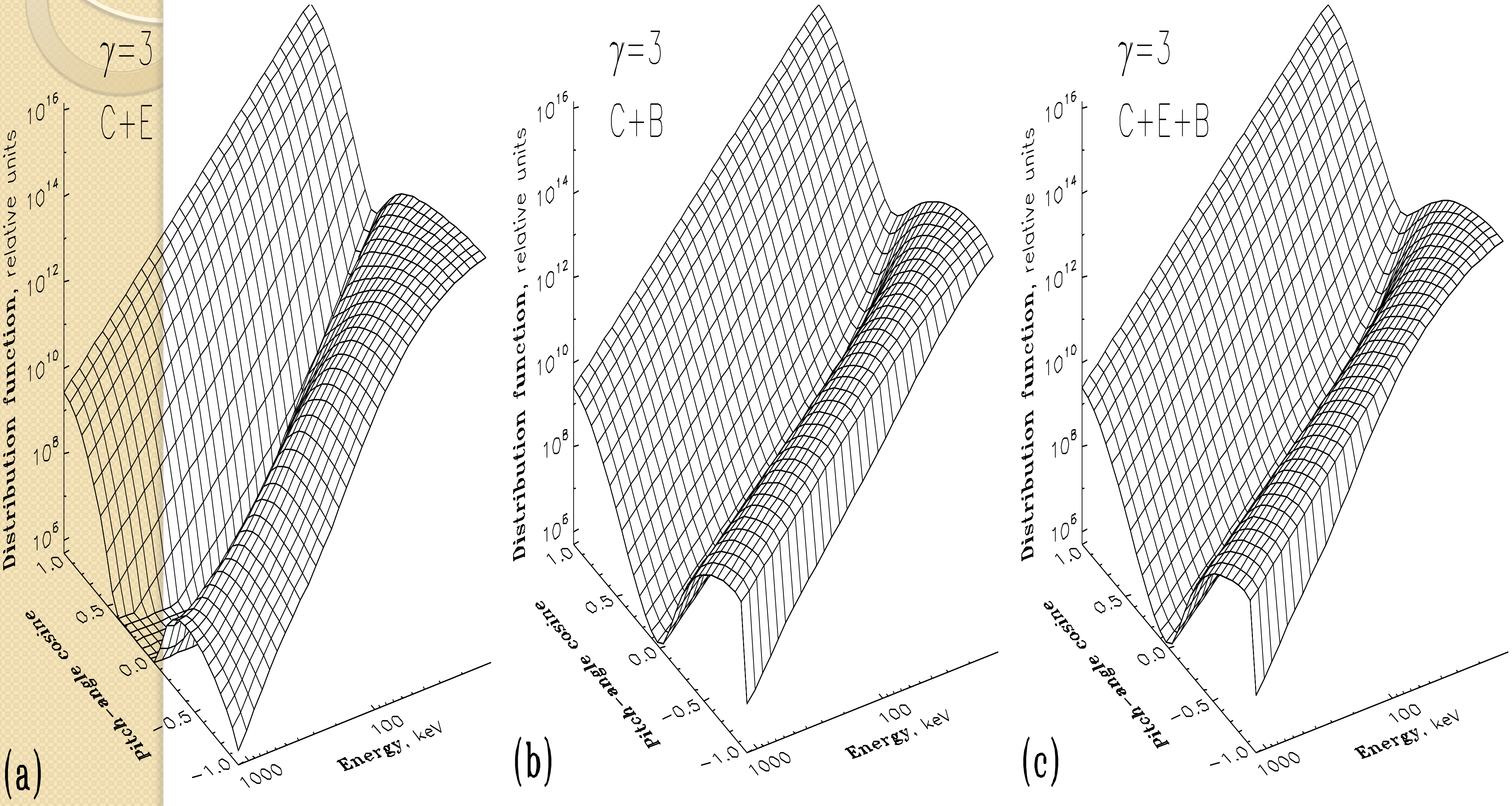

Electron distribution functions (quasi-stationary state) at $\xi=10^{20}$ cm^{-2}.

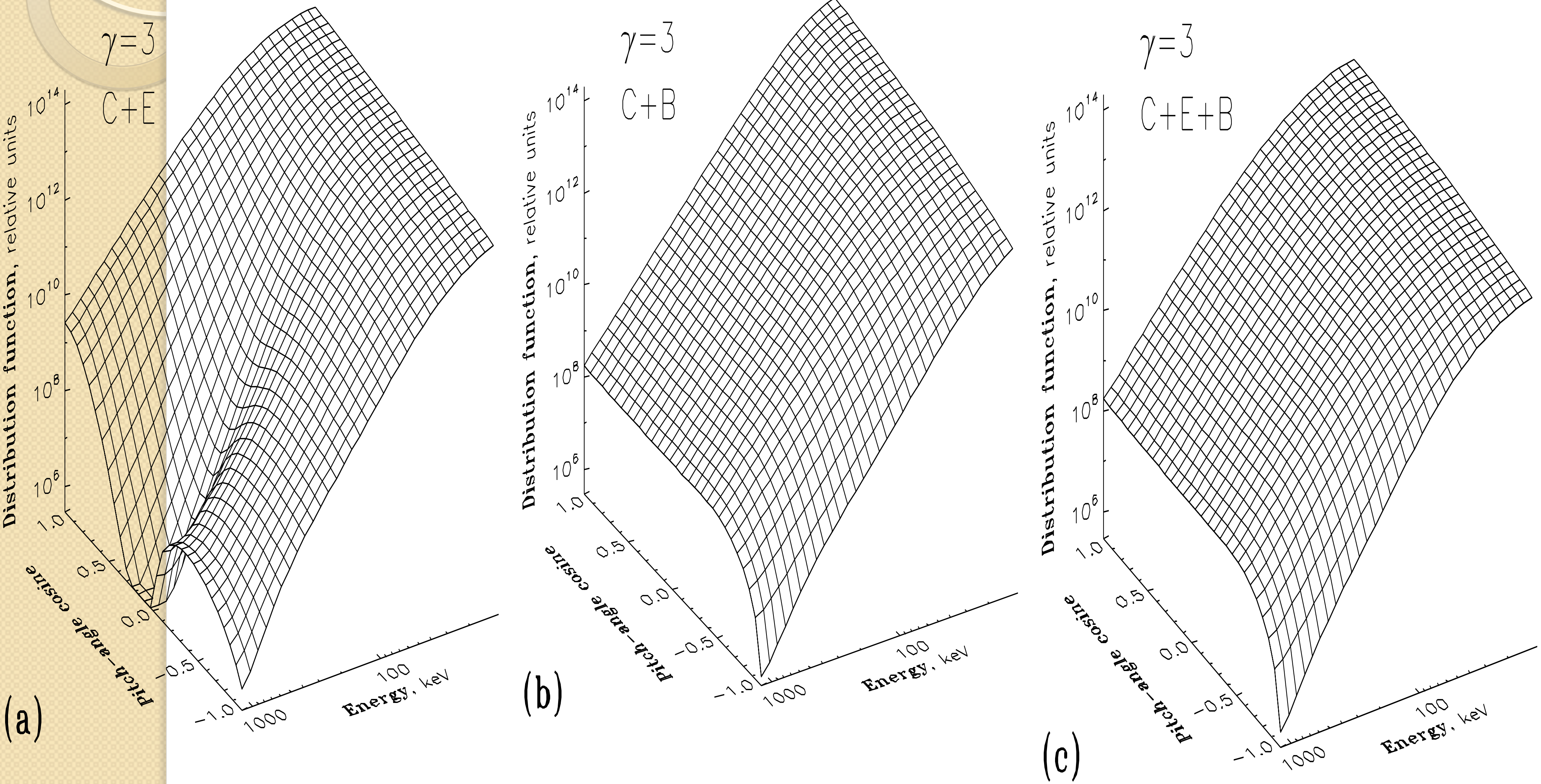

Depth variations of directivity and polarization

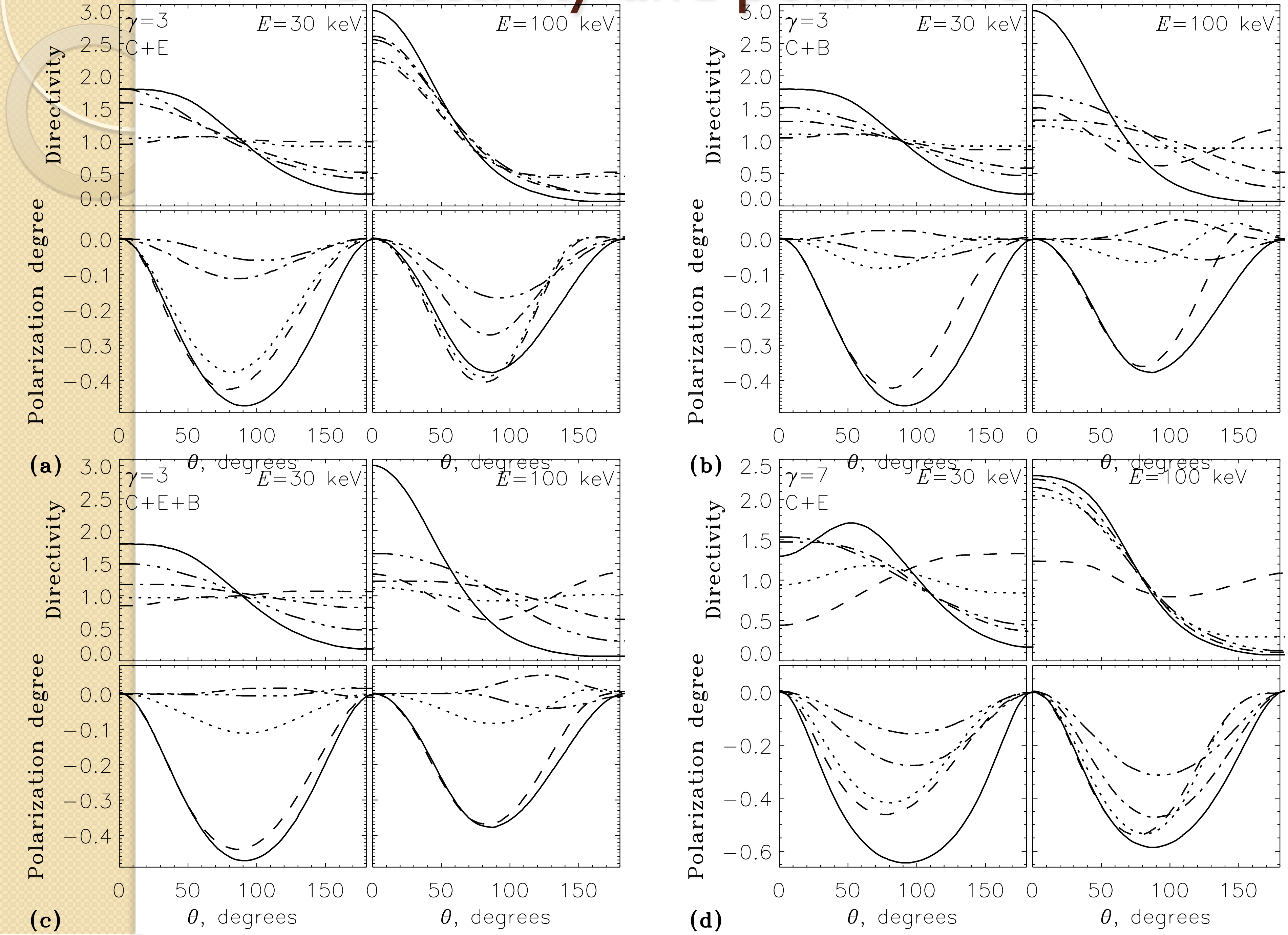

HXR emission at different heights and various viewing angles

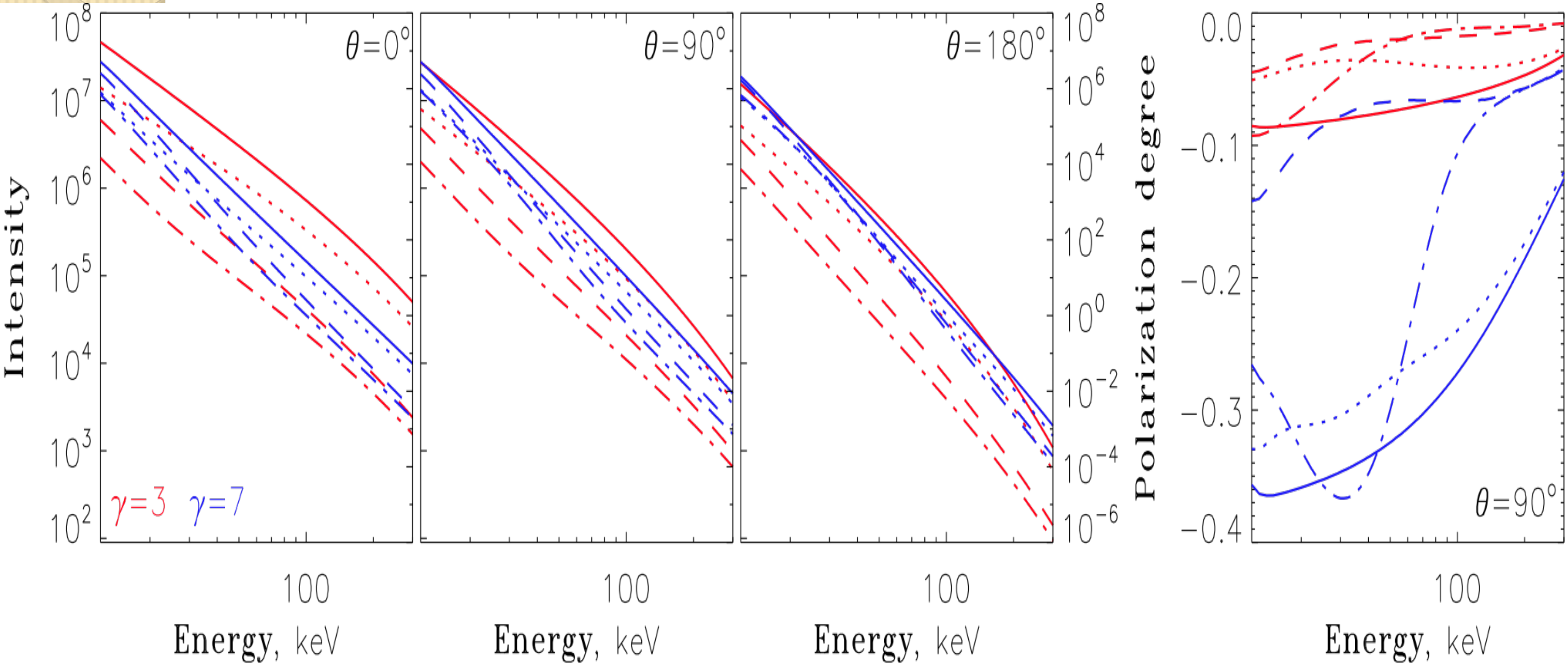

HXR photon spectra in flares

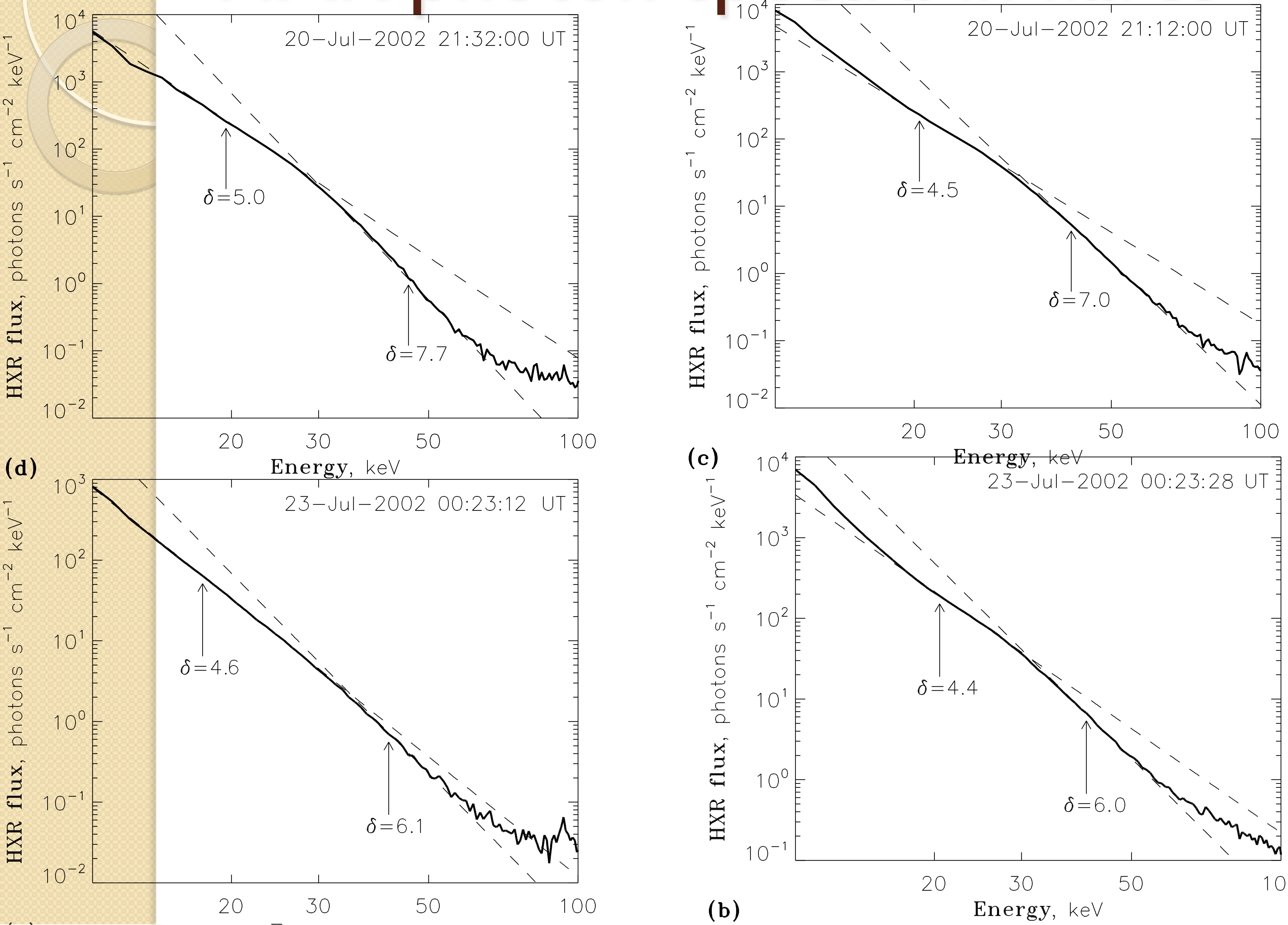

Photon energy spectrum and electron beam parameters RHESSI nugget 25, Zharkova et al, A&A, 2010

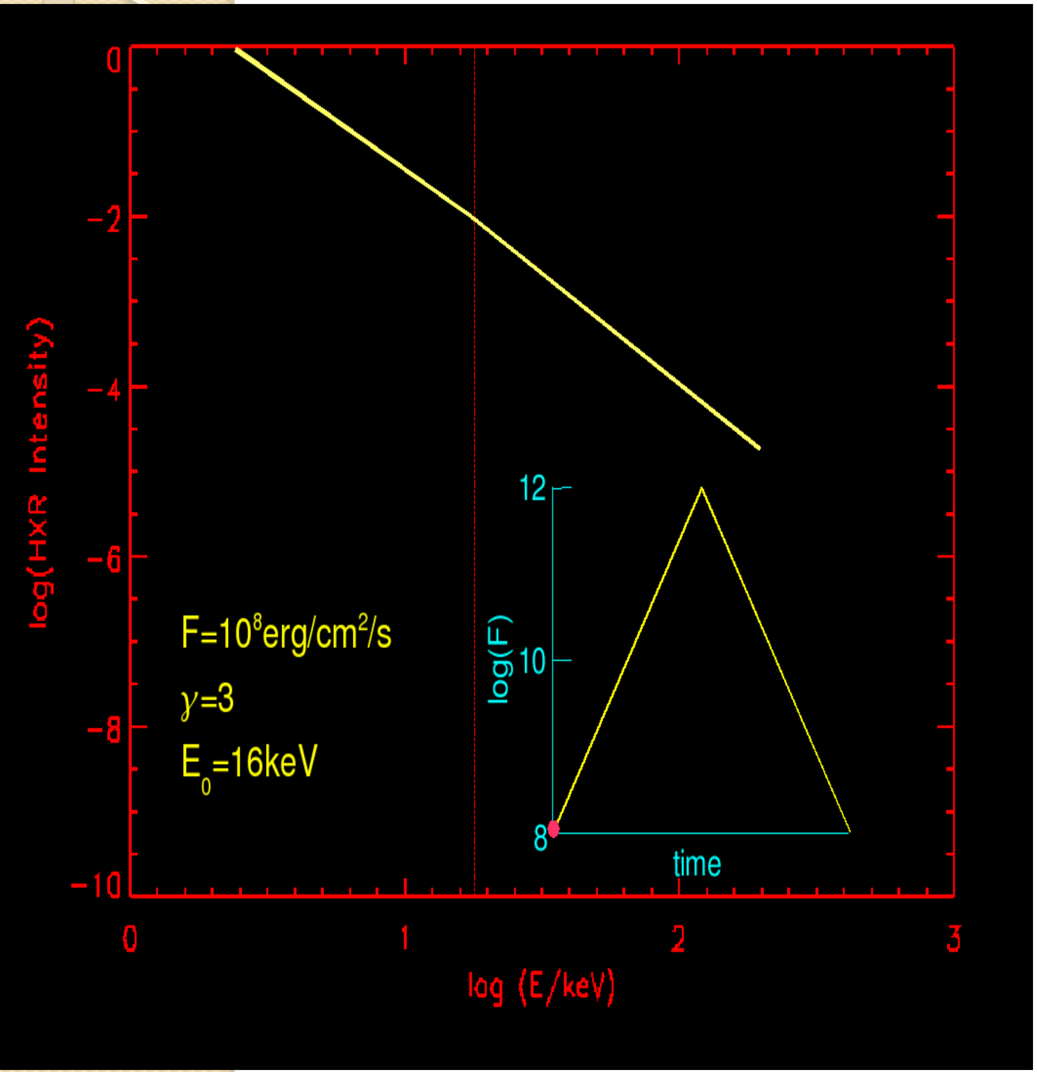

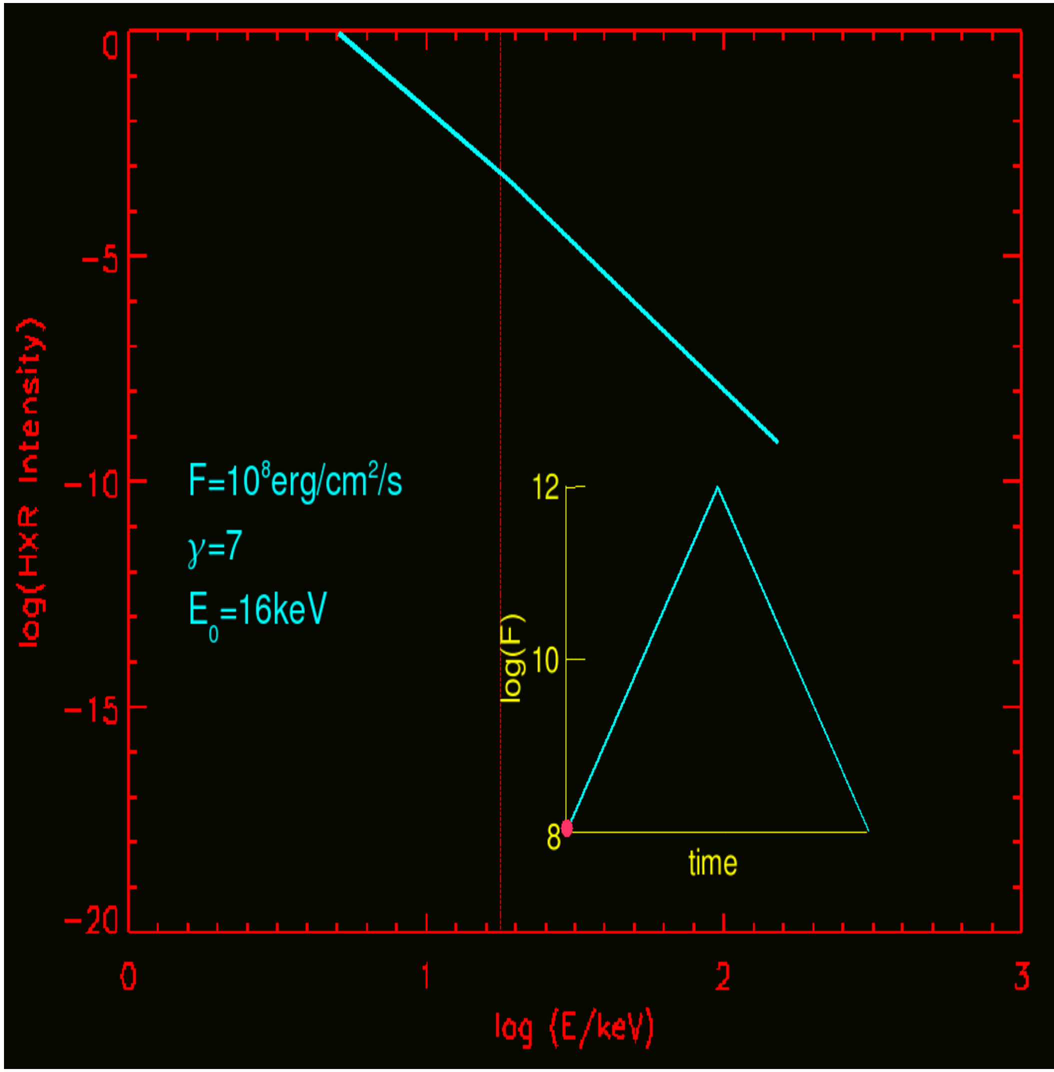

Observed directivity (150 flares, Kasparova et al., 2007) vs simulations (Zharkova et al, 2010)

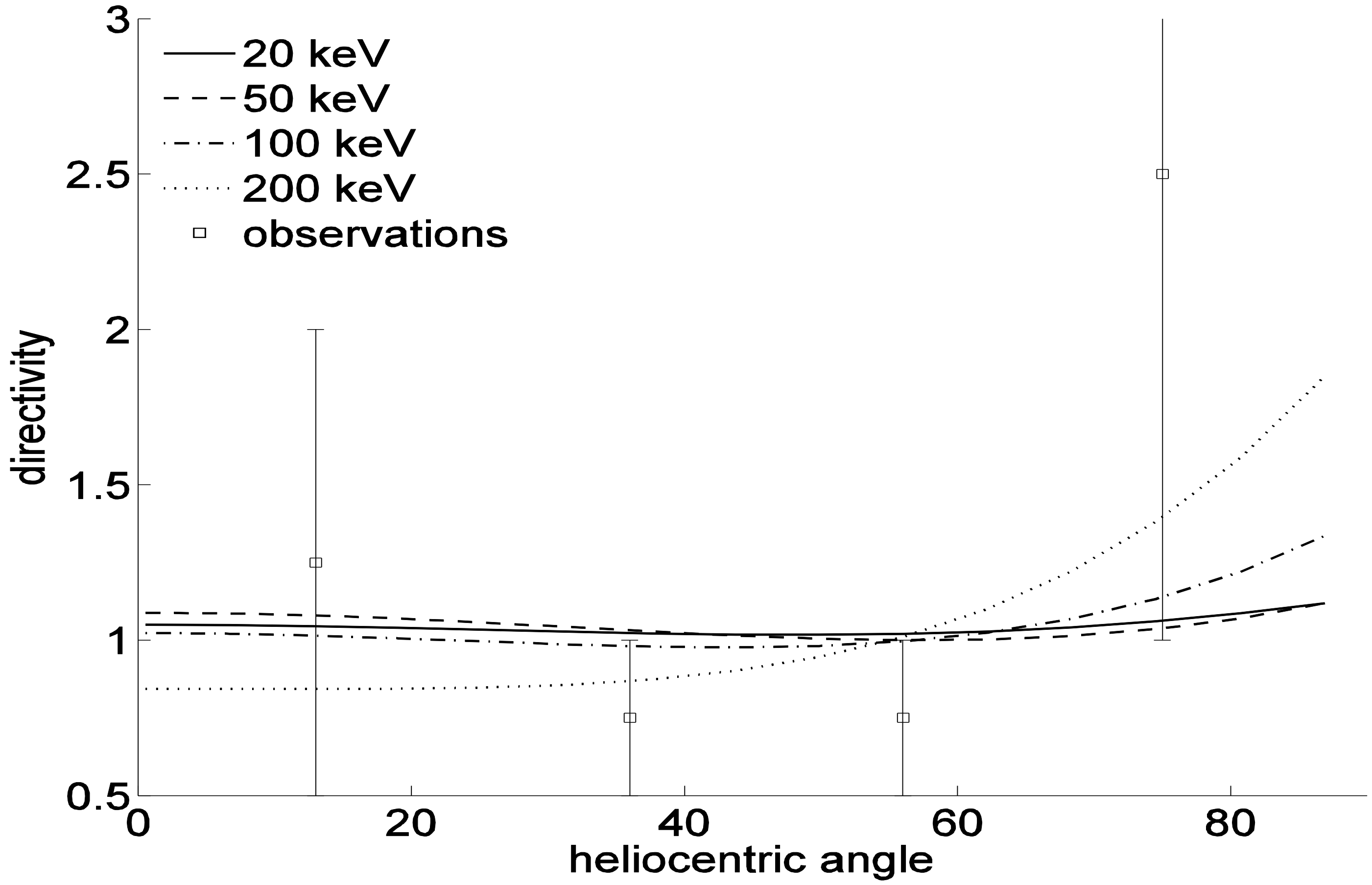

Observed polarization vs simulations

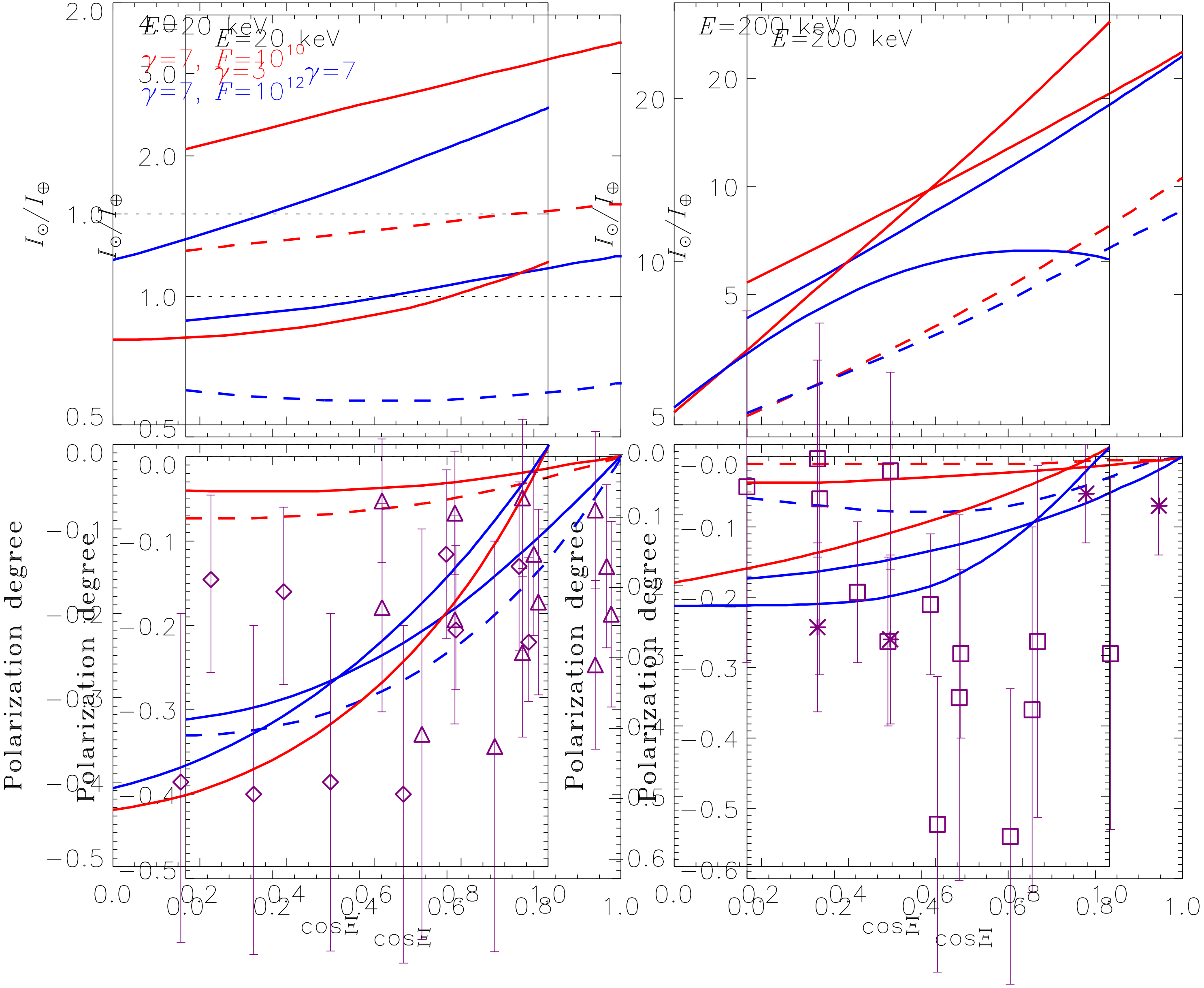

HXR polarisation in spherical Sun

Zharkova et al, 1995, A&A

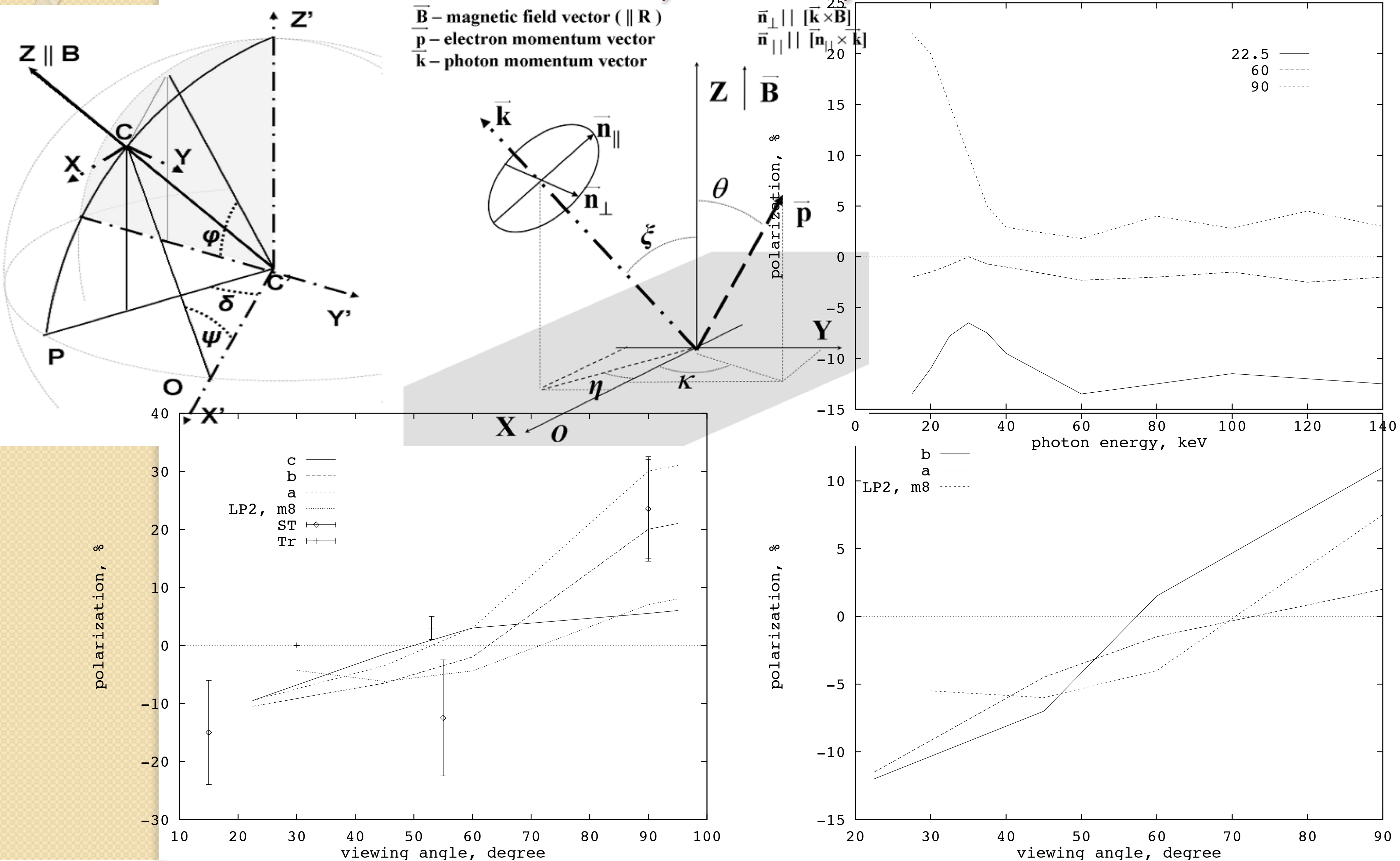

Polarization for different viewing angles

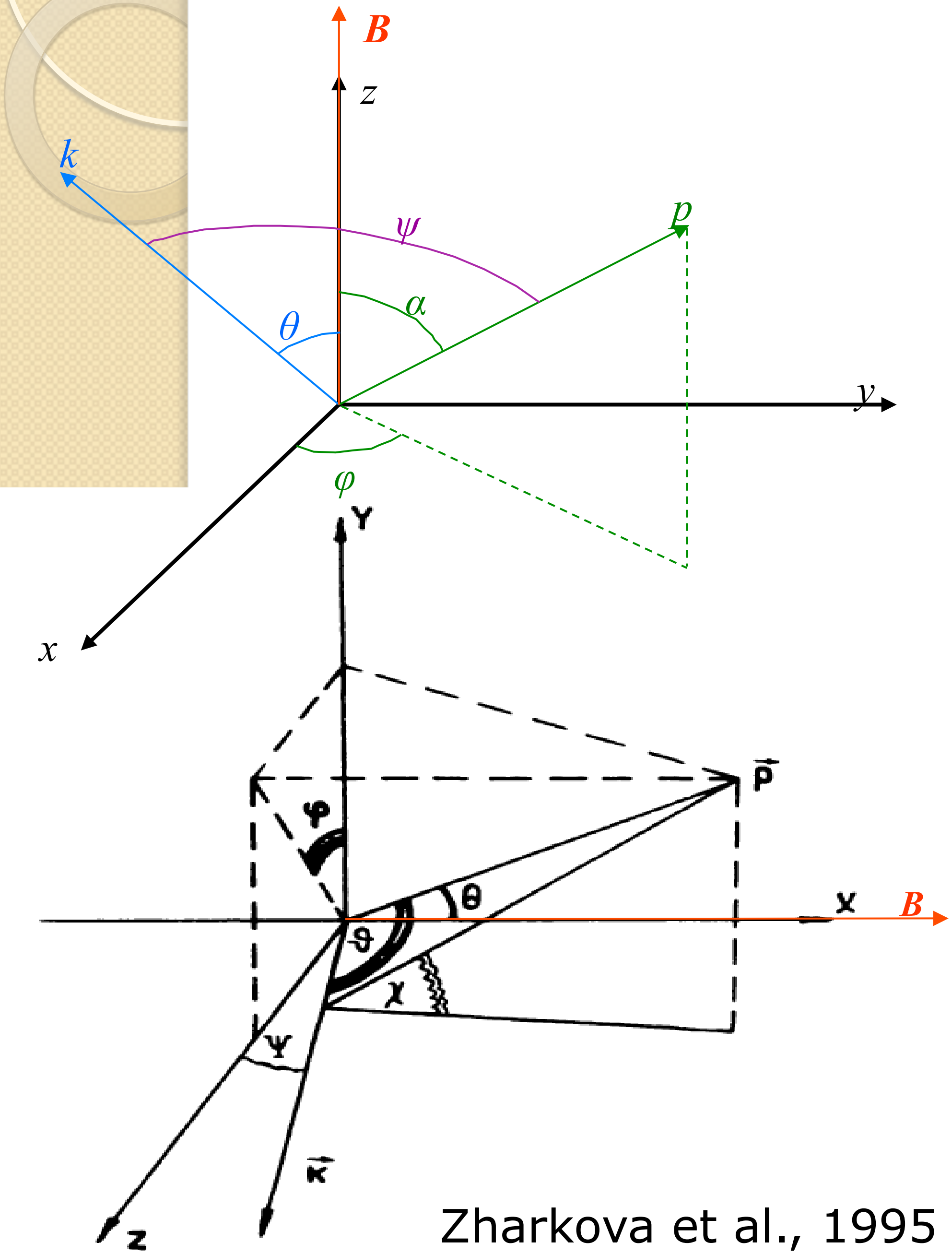

Zharkova et al., 1995

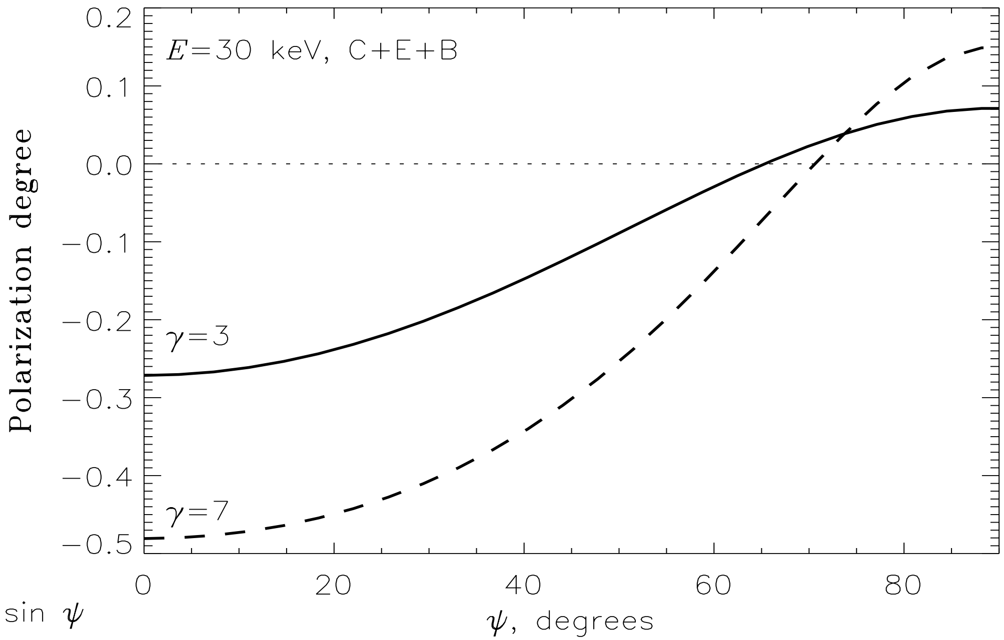

Summary

Stationary injection

- The relaxation time of the beam to reach a steady state injection is 0.07-0.2 s (the atmosphere is preheated by the beam with energy flux 10^{10} - 10^{12} erg cm^{-2} s^{-1}).
- The self-induced electric field increase a number of returning electrons with low and mid energy → electrons are recycled many times before they completely disappear.
- If the electric field is taken into account, the coronal heating becomes higher and the chromospheric heating becomes lower than in the case of the purely collisional precipitation.
- Convergence model proposed here can essentially reduce the corona and chromosphere heating.
- C+E+B model can explain HXR photon spectra, directivity and polarization observed in flares
- Important to consider sphericity of the solar disk, in order to simulate polarisation in flares occurring in active regions

Impulsive injection ($\Delta t = 1.7 \cdot 10^{-3}$s)

- The effect of the self-induced electric field is smaller when a short impulse is injected (in comparison to the steady injection).
- Maximum of the heating profile appears at the bottom and moves upwards, if the initial spectrum of the beam is hard enough.
- .If HXR photon counts allow (t<1s) the strongest polarisation can be observed